FACILITATED ION TRANSFER ACROSS THE MEMBRANE STABILIZED INTERFACE BETWEEN TWO IMMISCIBLE ELECTROLYTE SOLUTIONS

A Thesis Presented to the
School of Graduate Studies
Addis Ababa University

In Partial Fulfilment of
the Requirements for the Degree
of Master of Science in Chemistry

by

Leul Zeryihun

June 1993

Acknowledgements

I would like to express my deepest gratitude to my advisors Dr. Bernd Hundhammer and Dr. Theodros Solomon for their patience, deep concern and constant guidance throughout the course of this work. I would like also to extend my thanks to Dr. Hailemichael Alemu for his helpful discussions.

It is a great pleasure indeed to acknowledge my colleagues and friends Abebe G., Amare A., Ameha K., Atallo K., Genene, Hagos W/G, Hailemariam A., Haile G., Mohamoud M., Mussa K., Solomon M., Tsehaye A., Yeshitila G/M and others for their deep concern sympathy, encouragement, material and financial assistance.

My special thanks go to Gebre-Egziabher Kiros for making the final draft of the thesis ready in a very short period of time despite of his being overburdened and for his constant encouragement.

Finally, I would like to acknowledge Alemaya University of Agriculture for sponsoring my study.

Table of Contents

List of Figures

List of Table

Abstract

The transfer of Ni^{2+}, Cd^{2+} and Fe^{2+} facilitated by 2,2'-bipyridine and $Ni(bipy)_3^{2+}$ complex ion transfer across the membrane stabilized interface between two immiscible electrolyte solutions (water/nitrobenzene) was studied using the flow injection technique, and dc and ac cyclic voltammetry. In the flow injection analysis the dependence of peak current height on the applied potential all, with the exception of Ni^{2+}, showed an S-shaped polarographic wave with fairly sharp i-t curves, indicating the reversible or diffusion controlled transfer of these ions. Ni^{2+} showed poor current-potential dependence with a hardly discernible half-wave potential. The i-t curve was very broad which shows that the transfer of Ni^{2+} is kinetically controlled. Similarly the ac cyclic voltammogram of Cd^{2+}, Fe^{2+} and $Ni(bipy)_3^{2+}$ showed reversible behaviour with overlapping forward and reverse peak potentials and half-peak width of ~45 mv. In the ac cyclic voltammogram for the transfer of Ni^{2+} the peak potential for the forward and reverse scans did not overlap, indicating kinetically controlled transfer. The reversible transfer of the $Ni(bipy)_3^{2+}$ complex was studied by single sweep voltammetry and the diffusion coefficient of the ion in water was evaluated. In the ac voltammetric experiment only the transfer of the bis and tris complex was within the range of the potential window. The transfer of Ni^{2+} and Fe^{2+} are presumed to be a complex ion transfer while that of Cd^{2+} appears to be a facilitated ion transfer of Cd^{2+} may occur in the bulk phase. The change in standard Gibbs energy of transfer between the successive complexes of Ni^{2+} and Fe^{2+} was about 38.6 KJ/mol while that of Cd^{2+} was very large (53 KJ/mol).

1. INTRODUCTION

1.1. General

The early investigation of the interface between two immiscible electrolyte solutions (ITIES) dates back to the work done by Nernst & Riesenfeld [as quoted in ref.1]. These authors studied the transport of ions by passing electrical current through the system water /phenol/water.

Though bioelectrical studies begun with the work of Galvani (1878) followed by many other workers [for review see ref. 2], it was when Cremer [see ref. 1] explained the analogy between the water /oil/ water cell and the biological membrane that physiologists were attracted. No significant progress was made in the attempt to model biological membranes until recent years [3]. ITIES is the simplest of the model systems representing one half of the biological membrane. Others include the thick liquid membrane, interface between an aqueous electrolyte solution and non-conducting liquid, and the more popular bilayer lipid membrane. The use of simple models are believed to be of paramount importance in the understanding of the more complicated biological membrane processes. Insertion of an artificial membrane [4] which can be chemically modified and the presence of adsorbed amphiphilic substances such as phospholipids and proteins [see ref. 5] at the ITIES are thought to give a more

realistic picture of the biological membrane. Furthermore ITIES can be exploited in analytical chemistry, for example, in the direct determination of ions [6,7], assay of ionophores [8], determination of ions facilitated by ionophores [9], etc. Studies at the ITIES are also important in understanding the behavior of ion-selective electrodes (ISE) [10,11], in separation science such as solvent extraction [12], phase transfer catalysis [13] and photochemical energy conversion.

Early development of the studies at the ITIES was very slow as compared to the metal electrode electrolyte solution interface. Until the mid-fifties the investigation of ITIES was limited to the study of steady state electrical potential differences between water and organic phases in the presence of different electrolytes. For decades there has been controversy over the origin of the potential difference. Cremer (1906) explained this in terms of diffusion potential; Beutner (1912) claimed it to be due to free charge located at the oil water interface as a result of unequal distribution of ions in the two phases and Bauer (1918) interpreted it as originating from selective ion adsorption at the interface. Finally Beutner's suggestion was found to be correct [for review see refs. 1 and 17].

The thermodynamics of the ITIES was treated in detail by Karpfen and Randels [15] and Sollner and Shain [16].

A breakthrough came when experiments begun to be carried out under flow of current [18,19]. The effect of current flow on the interfacial potential difference and the phenomenon of electroadsorption (from the change of interfacial tension) was investigated by many workers [for review see ref. 2,16]. Blank [20] showed that the phenomenon of electroadsorption was due to accumulation and depletion of surface active species at the interface.

Modern electrochemical methods for the investigation of ITIES had their root with the work of Gavach et al. [21]. These authors showed that the ITIES can be polarized. Gustalla [21] applied a triangular voltage and recorded the current response of the system KCl (a hydrophilic salt), dissolved in the aqueous phase and tetradecyl trimethyl ammonium picrate (hydrophobic salt) in the organic phase. Chronopotentiometric studies were also carried out [23-26]. These authors analyzed their results using the well established theoretical framework for the metal electrolyte solution interface.

Among the thermodynamic quantities that are sought is the standard Gibbs energy of transfer, ΔG_{tr} , of an ion between aqueous and organic phases, which is a reflection of the difference in the solvation Gibbs energy of an ion between the two phases. Data on the standard Gibbs energy of transfer from partition measurements are given by Rais [27]. An updated

version is given in reference 17. Electrochemical methods have also been used to determine ΔG_{tr} [for eg. see ref. 28]. The standard Gibbs energy of transfer can also be predicted theoretically. A review of the theoretical models for the estimation of the Gibbs energy of transfer is given in ref. 14. The model of ionic solvation energy which is widely used is due to Abraham and Liszi [29,30].

The most commonly used organic solvents are nitrobenzene and 1,2 dichloroethane. The choice of the organic solvent is limited by the following requirements. First, the mutual solubility of the organic phase and aqueous phase in each other should be very small. Second, the organic solvent must provide enough conductivity, that is, it should be sufficiently polar for the dissociation of the base electrolyte (ε >10). Thirdly, the difference in density between the aqueous and organic phase should be large enough so as to form a physically stable interface. Nitrobenzene is a solvent that meets all the requirements. Despite its lower permittivity than nitrobenzene, 1,2 dichloroethane [31] shows a somewhat wider potential window [2]. Besides these solvents acetophenone [32], isobutylmethyl ketone [34], o-nitrotoluene [14], benzonitrile [14] and o-dichlorobenzene [14], and organic mixture of solvents such as nitrobenzene-benzonitrile [35], nitrobenzene - chlorobenzene [36] and nitrobenzene- benzene [35] have been studied. The choice of

solvent limits the potential range in which the interface is polarized. In addition to the type of solvent the kind of supporting electrolyte used in both the aqueous and organic phases play an important role in determining the potential window. In order to get wider useful potential windows the base electrolyte in the aqueous phase should be very hydrophilic and the base electrolyte in the organic phase should be very hydrophobic.

The most commonly used organic supporting electrolytes are tetraphenyl arsonium tetraphenyl borate (TPAsTPB), tetrabutyl ammonium tetraphenyl borate (TBATPB), crystal violet tetraphenyl borate (CVTPB), μ- nitro-bis (triphenyl phosphorus)- 3,3-bis (undercahydro-1,2-dicarba-3-cobaltaclosododecabor) ate (PNPDCC) and other tetraalkyl ammonium tetraphenyl borates (TAATPB).The Crystal violet cation extends the polarization window to a more negative potential enabling the study of anions. The most negative potential so far reached was with the system: NaF in the aqueous phase and crystalviolet tetraphenyl borate in nitrobenzene [37]. Moreover, salting out of the salts formed of organic ions widens the potential window when the transfer of these ions limit the width of the potential window [38].

In 1979 Koryta compared the faradaic and non faradaic processes occurring in the metal/electrolyte solution interface with that of the ITIES. Further, he showed that with a proper experimental

setup the ITIES is an analogue of the metal electrode electrolyte interface and that the ITIES could be studied by methods analogous to those used with metallic electrodes [2].

As described in ref. 17 the difference between the two interfacial processes is that at the ITIES,

(a) diffusion - migration via the Nernst - Plank equation rather than Fick's first law must be considered.

(b) interfacial transport of ions of opposite sign must be considered because of salt partition equilibria.

(c) partition equilibrium is a non-linear ionic process that can lead to insoluble equations.

The electrochemical methods used for the investigation of ion transfer at the ITIES include, chronopotentiometry [18] dc cyclic voltammery [39], ac cyclic voltammetry [40] linear sweep voltammetry [48], convolution potential sweep voltammetry [49,50], semi-differential cyclic voltammetry [8], differential pulse stripping voltammetry [52,54], current scan polarography [41], electrolyte dropping electrode [42,43], potential step chronoamperometry [51], and a flow injection technique based on amperometeric detection [9]. The capacitance of the interface has been evaluated from impedance measurements with phase selective ac polarography and an alternating bridge [44] and from surface tension measurements [46, 47]. The galvanostatic pulse method has been utilized in the evaluation of capacitance and ohmic potential drop [40]. Apart from the simple L/L interface membrane

stabilized ITIES [9] and polymer-gel liquid interface's [53,55] have been utilized.

1.2. The Electrical Double Layer

At the ITIES there is an excess electrical charge on one side of the interface which has to be compensated for by excess opposite charge on the other side for electroneutrality to be attained. Such a charge separation gives rise to the electrical double-layer. One of the objectives in studying the ITIES is to establish its structure, which in turn enables one to understand the rate and mechanism of charge transfer across the interface. Great effort has been devoted to both theoretical and experimental investigation of the structure of the electrical double layer formed at the ITIES. Experimentally the structure of the double-layer at the ITIES was inferred from surface tension [46,47,56,58] and capacitance measurement [45,59,63].

In 1977 Gavach et al. [47], by analogy with Stern's modification of the double layer at the metal electrode solution interface, introduced a model of the ITIES with a compact layer (inner layer) of oriented solvent molecules (in the absence of specific adsorption) with two diffuse layers. This model, known as the modified Verwey and Niessen (MVN) model, is an extension of the Verwey and Niessen (VN) model, which assumes no compact layer; instead it assumes that the double layer charge (the Galvani

potential difference) appears completely within the two diffuse layers [5]. Discrepancy from the MVN was observed by different investigators [59,64]. Samec et al. [59] found the MVN description of the diffuse layer to be inadequate. Based on surface excess measurements [58] Girault and Schiffrin argued that there is no inner layer of oriented solvent molecules, hence, no interfacial potential drop. Instead they suggested that the inner layer is a thin mixed solvent layer with a continuous change in composition from one phase to another [72]. On the contrary Samec says that the liquid-liquid boundary is sharp, i.e., a drop or rise in density of one or the other solvent respectively occurs at a molecular distance [65]. Samec et al. [63] attempted to explain the discrepancy from the MVN theory, considering the MVN model in which ions were allowed to penetrate into the inner layer. Different approaches to the double layer structure were also presented by different authors [66,67].

1.3. Ion-Transfer Kinetics

The study of the kinetics and mechanism of ion transfer is dependent on the model of the ITIES used. So far there is no unequivocal model that can be applied under all conditions. Therefore, despite the great wealth of information that has been accumulated, a detailed understanding of the mechanism and rate of ion transfer is lacking.

Kinetic analysis which accounts for the ion distribution across the ITIES was carried out for the transfer of TAA^+ [62,68], picrate [69], Cs^+ [50] alkaline earth metal cations facilitated by polyether diamides [70], Na^+ facilitated by dibenzo -18-crown-6 [71] and electron transfer between ferrocene and hexacyanoferrate (III) [50]. In most theoretical kinetic treatments the simple VN model is assumed as the approximate picture of the ITIES [72-73]. The second way is based on the modified VN model where, for the ion transfer a potential dependent step of transfer across the inner layer is also taken into account [73-67].

1.4. Charge Transfer

Charge transfer at the ITIES involves simple and facilitated ion transfer as well as electron transfer between redox couples located in each phase.

Ion transfer across an organic/water interface is fast, so that, in most cases they are reversible and diffusion controlled. Diffusion controlled electrochemical measurements enable the evaluation of diffusion coefficients and thermodynamic quantities such as the Gibbs energy of transfer.

1.4.1. Simple Ion Transfer

Simple ion transfer has been researched extensively. The transfer of the tetramethyl ammonium ion was studied by Samec [74]

employing the polarographic technique using an ascending electrolyte dropping electrode. Cyclic voltammetry was used to study the transfer of Cs^+ and TBA^+ [74]. The transfer of TMA^+ and picrate was studied using chronopotentiometry [2]. Similarly the transfer of the following ions has been investigated: choline and acetyl choline [75], TMA^+ [76] TEA^+ [77,78], dialkyl viologen and tris-dipyridine ruthenium (II) [33], Li^+, Na^+, K^+, Rb^+ and Cs^+ [79], Li^+, Na^+ Rb^+, Cs^+ [80]. In almost all cases a reversible diffusion controlled transfer was observed.

In an analogous manner the study of anion transfer such as picrate [28,40,81-76,78], ClO_4^-, SCN^-, NO_3^- [76] for which the transfer of the ions only from nitrobenzene to water was within the potential window was investigated; n-octoate, laurylsulfate, perchlorate and thiocyanate [82] were studied using the electrolyte dropping electrode (EDE). The transfer of halides and their oxoacids viz. Br^-, I^-, IO_4^-, ClO_4^-, ClO_3^-, ClO_2^- and the ions CN^-, BF_4^-, $Cr_2O_7^{2-}$, NO_3^-, and NO_2^- were investigated by current Scan polarography with EDE [83]. The authors reported that the transfer of most of the ions was reversible and hence diffusion controlled. They also related the half-wave potential to the inverse of the thermochemical radii of the ions. Hundhammer and Solomon [28] studied the reversible transfer of I^-, ClO_4^-, NO_3^-, SCN^-, IO_4^- and BF_4^-, using dc cyclic voltammetry. The transfer behavior of I^- and its complexes with iodine (I_3^- and I_5^-) was discussed by Zhicheng & Erkang [84]. The transfer of Bromocresol

Green, a weak acid dye, was also studied [85]. In addition to the simple organic solvent water interface the membrane stabilized interface has also been utilized for the study of the transfer of anions [7]. The transfer of ions across the polyvinylchloride-nitrobenzene gel/aqueous electrolyte interface was studied [86,53]. These include acetyl choline (Ach^+), methylviologen (Mv^+), Cs^+, picrate (pi^-), ClO_4^- [86] and potentiometric stripping analysis of Cl^-, SCN^- and NO_3^- [53].

1.4.2. Facilitated ion transfer

As described elsewhere the available potential window and therefore, the number of ionic species which can be transferred across the ITIES is limited. However, the transfer of an ion whose transfer potential would normally be outside the accessible potential window can be studied in the presence of an ionophore in the organic phase. The ionophore facilitates the transfer. An ionophore is a strongly hydrophobic compound capable of complexation with ions resulting in the formation of hydrophobic complex [2,5]. In 1979 Koryta using cyclic voltammetry showed, that the transfer of alkali metal ions (K^+ & Na^+) can be facilitated in the presence of dibenzo-18-crown-6 and valinomycin [2]. The transfer of sodium with monensine [87] and nonactin [88] was also studied. In these studies the concentration of the ionophore in the organic phase was much smaller than that of the metal ion in the aqueous phase, in which case diffusion

controlled transfer was observed. In some cases [87] the stability constant of the complex was evaluated. Koryta [2] assumed that the complexation takes place in the organic phase after the transfer of the metal ion to the non-aqueous phase. Freiser and Yoshida also studied the same system, i.e., the facilitated transfer of K^+ using valinomycin [89] and dibenzo-18-crown-6 [90,91], but using different electrochemical methodology. These authors used polarography at an ascending water electrode (AWE) and chronopotentiometry at a stationary electrode. They argued that at low potassium ion concentration the complexation takes place in the aqueous phase after the ionophore is transferred to the aqueous phase. When the concentration of K^+ is high they suggested that complex formation takes place at the interface. They also studied the transfer of K^+ facilitated by a polymer urushiol crown ether in the organic phase [91]. The problem of establishing the elementary rate determining step was also studied by Senda et al. and Taylor & Girault [70,92]. These investigators suggested that the complexation reaction occurs at the interface. Facilitated ion transfers have also been observed using the hanging electrolyte drop electrode (HEDE) for alkaline earth metals using 7,19-dibenzyl-2,3-dimethyl-7,9-diaza-1,4,10,13,16 pentaoxacycloheneicosane-6,20-dione (PEDA) [93]. The possible use of HEDE in quantitative analysis was shown, employing differential pulse stripping voltammetry, by Homolka et al. [94] who studied the facilitated transfer of Ca^{2+} by a synthetic

neutral macrocyclic ether. The stoichiometry of assisted ion transfer was evaluated experimentally by Homolka et al. [95] using the theory for single scan voltammetry. The transfer of alkali and alkaline earth metal ions facilitated by polyoxyethylene ether (Triton-x) was investigated [99]. The complex ion transfer of Fe^{2+}, Ni^{2+} and Zn^{2+} with 2,2'-dipyridine and o-phenanthroline was studied by Homolka & Wendt [96]. Facilitated transfer of Cd^{2+} by 2,2'-dipyridine was observed by Ruixi & Xiaping [8] and Wang & Liu [97]. Both groups observed the transfer of the 1:2 (metal to ionophore) complex ion. The former used semi-differential cyclic voltammetry while the latter used chronopotentiometry with cyclic linear current scanning. Liu & Wang [98] also studied the transfer of Co^{2+} facilitated by 2, 2'-bipyridine using cyclic voltammetry. They observed the transfer of the successive complexes of cobalt (II) viz. 1:1, 1:2 & 1:3 Co to bipyridine. They suggested that successive complexes of Co^{2+} are formed in a coupled chemical reaction in the organic and aqueous phases during an electrochemical transfer. Very recently [14] complex ion transfer of Fe^{2+}, Co^{2+}, Co^{3+}, Ni^{2+}, Zn^{2+} and Cu^{2+} with terpyridine and facilitated ion transfer of Cu^{1+} using 2, 2'-biquinoline was studied using ac cyclic voltammetry and absorption spectroscopy. The relative stabilities of the mono and di terpyridine complexes were discussed. A mechanism for the irreversible Cu^{1+} transfer facilitated by 2, 2'-biquinoline was proposed.

The facilitated transfer of the proton (H^+) by monensin was studied by Koryta [100]. Homolka [101] studied the transfer of H^+ facilitated by aniline and o-phenanthroline. Facilitated proton transfer using tetracycline and its derivatives has also been investigated [see Ref. 5]. Very recently the facilitated transfer of H^+ using 1,10-phenanthroline was studied using current linear sweep voltammetry [102].

1.5 Scope of the Present Work

The objective of the present study was to investigate the facilitated transfer of cations across the membrane stabilized interface between two immiscible electrolyte solutions, particularly to study the transfer of the transition metal ions (Cd^{2+}, Ni^{2+}, Fe^{2+}) facilitated by 2,2'-bipyridine employing dc and ac cyclic voltammetry as well as the flow injection technique.

2. THEORY

For two immiscible solvents such as water(w) and organic(o) solvent in contact each containing ions of species i under equilibrium condition the electrochemical potential of the species $\tilde{\mu}_i$ in both phases should be equal, i.e.,

$$\tilde{\mu}_i(w) = \tilde{\mu}_i(o) \qquad (1)$$

$$\mu_i^{\circ}(w) + RT \ln a_i(w) + z_i F\varphi(w) = \mu_i^{\circ}(o) + RT \ln a_i(o) + Z_i F\varphi(o) \qquad (2)$$

where μ° is the standard chemical potential, a is the activity and $\varphi$is the Galvani (inner) potential and other symbols have their usual significance.

The Galvani potential difference, $\Delta_o^w\varphi$, formed at the interface is given, from Eq. (2), by

$$\Delta_o^w\varphi = \varphi(w) - \varphi(o) = (\mu_i^{\circ}(o) - \mu_i^{\circ}(w))/zF + \frac{RT}{z_i F} \ln \frac{a_i(o)}{a_i(w)} \qquad (3)$$

Substituting the relation for the standard Gibbs energy of transfer of the ionic species i from water to the organic phase, $\Delta G_{tr}^{w,\rightarrow o}$,

$$\Delta G_{tr}^{o\ w\rightarrow o} = \mu_i^{\circ}(o) - \mu_i^{\circ}(w) \qquad (4)$$

we get

$$\Delta_o^w\varphi = \frac{\Delta G^{o\,w\to o}}{z_i F} + \frac{RT}{z_i F} \ln \frac{a_i(o)}{a_i(w)} \qquad (5)$$

$$\Delta_o^w\varphi = \Delta_o^w\varphi^o + \frac{RT}{z_i F} \ln \frac{a_i(o)}{a_i(w)} \qquad (6)$$

where $\Delta_o^w\varphi^o$ is the standard Galvani potential difference expressed as

$$\Delta_o^w\varphi^o = \frac{\Delta G_{tr}^{o,w\to o}}{z_i F} \qquad (7)$$

The influence of the solvent is incorporated in the standard chemical potential.

Thermodynamic quantities for a single ion, such as the Gibbs energy of transfer, partition coefficient, and Galvani potential difference are not accessible to direct measurement. For a quantitative measurement to be possible an extrathermodynamic assumption must be made. Different assumptions have been proposed [1]. Frequently the tetraphenyl arsonium tetraphenyl borate (TATB) assumption is applied [103]. This assumption states that both the cation and anion of tetraphenyl arsonium tetraphenyl borate have equal Gibbs energy of transfer in any pair of solvents, i.e.,

$$\Delta G_{tr,TPAS^+}^{o,w\to o} = \Delta G_{tr,TPB^-}^{o,o\to w} = 1/2\ \Delta G_{tr,TPAS\ TPB}^{o,o\to w} \qquad (8)$$

Based on this assumption the standard Gibbs energy of transfer of an ion can be obtained from electrochemical measurement and

from standard Gibbs energy of transfer of salts which are evaluated from partiton constants.

2.1 Polarization Phenomena

Polarization at ITIES is a process by which a relative displacement of positive and negative charges takes place at the **interface when an electric field is applied.**

2.1.1. Unpolarizable ITIES

In a perfectly unpolarizable interface there is unhindered exchange of ions between the two phases, therefore ionic equilibrium for all the ionic species prevails throughout the system. The Galvani potential difference established in this kind of system is known as the distribution potential. Let us consider an electrolyte B_1A_1 distributed between water(w) and organic(o) phases [15]

$$A_1B_1\ ^{w} \mid A_1B_1\ ^{o} \qquad (9)$$

At equilibrium the electrochemical potentials of each ion in both phases is equal, that is,

$$\mu_{B_1^+}(w) = \mu_{B_1^+}(o)$$

$$\mu_{A_1^-}(w) = \mu_{A_1^-}(w) \qquad (10)$$

for which the Galvani potential difference is expressed by

$$\Delta_o^w\varphi = \Delta G^{o\ w\to o}_{tr,B_1^+} + \frac{RT}{F}\ln\frac{a_{B_1^+}(o)}{a_{B_1^+}(w)} \qquad (11)$$

$$= -\Delta G^{o\ w\to o}_{tr,A_1^-} + \frac{RT}{F}\ln\frac{a_{A_1^-}(o)}{a_{A_1^-}(w)}$$

For a dilute solution, ($a_i \approx c_i$) it can be shown that

$$\Delta_o^w\varphi = 1/2\,(\Delta G^{o,w\to o}_{tr,B_1^+} - \Delta G^{o,w\to o}_{tr,A_1^-}) \qquad (12)$$

The distribution potential for more electrolytes distributed between two immiscible phases was derived by Hung et al [104]. The potential difference established at the ITIES when at least one of the ions remains exclusively in one of the phases (termed the Donnan potential) has also been treated [1].

2.1.2. Ideally Polarizable ITIES

The characteristic of an ideally polarized ITIES is the absence of exchange of ions between the two phases.

Consider a system with the electrolyte A_1B_1 is practically confined to water and A_2B_2 to the organic phase [2].

$$A_1B_1^{+\ w} \mid A_2B_2^{\ o} \qquad (13)$$

The equilibria of the exchange processes

$$A_1^-(w) + A_2^-(o) = A_1^-(o) + A_2^-(w) \qquad (14)$$

$$B_1^+(w) + B_2^+(o) = B_1^+(o) + B_2^+(o)$$

are strongly shifted to the left hand side. Under this condition the potential difference is determined more by the charge in the double layer (which can be changed by charging the phases from an external source) rather than by the very small activities of the ion ($a_{A1}^-(o)$, $a_{A2}^-(w)$, $a_{B1}^+(o)$ and $a_{B2}^+(w)$). In other words the standard potential of transfer of the cation in the aqueous phase (B_1^+) and the anion in the organic phase (A_2^-) are very positive and the transfer potential of the anion in the aqueous phase (A_1^-) and cation in the organic phase (B_2^+) are very negative. Consequently there will be a potential range for which the potential of the interface is set at will by an external voltage source, i.e, the ITIES is polarized.

2.2 Gibbs energy of transfer

The standard Gibbs energy of transfer, which is the difference in the solvation energy of an ion in the water and organic phase, is given by Eqn. (4),

$$\Delta G_{tr}^{w\to o} = G_{solv}^{o}(o) - G_{solv}^{o}(w)$$

The Gibbs energy of transfer refers to the transfer of the anion from a pure water solvent into a pure organic solvent. It is therefore different from the Gibbs energy of partition (ΔG_p) which refers to the transfer of an ion from water saturated with the organic phase to the organic phase saturated with water. For a pair of solvents of low miscibility, such as water/nitrobenzene and water/1,2 DCE, the Gibbs energy of partition is equal to the Gibbs energy of transfer, showing that ions are not hydrated in the organic phase, exceptions being ions with very high ionic potential such as Li^+ and F^- which are strongly hydrated. For these ions the standard Gibbs energy of transfer is higher than the Gibbs energy of partiton [29]. The same is true for partially miscible solvent systems.

Prediction of the Gibbs energy of solvation of an ion using a theoretical model is useful for knowing the state of the ion transferred and to estimate the Gibbs energy of transfer in the absence of experimental data. Among the theoretical models that have been proposed is the model by Abraham & Liszi [29,30,105-108]. According to these authors the standard Gibbs energy of solvation, ΔG_s°, of an ion can be split into an electrical contribution ΔG_e°, and a neutral contribution ΔG_n^o, i.e.

$$\Delta G_s^o = \Delta G_n^o + \Delta G_e^o \qquad (15)$$

where ΔG_e^o is the electrostatic energy of interaction of the ion with the solvent and ΔG_n^o is the Gibbs energy of solvation of a non-polar gaseous solute of the same size as the ion in question including the cavity formation term.

For an ion unhydrated in the organic phase the electrostatic energy term is given by

$$\Delta G_e^o = \frac{N(ze)^2}{8\pi\varepsilon_o}\left\{\left(\frac{1}{\varepsilon_1} - 1\right)\left(\frac{1}{a} - \frac{1}{b}\right) + \left(\frac{1}{\varepsilon_o} - 1\right)\frac{1}{b}\right\} \qquad (16)$$

where b-a is the thickness of the first organized solvent layer surrounding the ion, ε_1 is the dielectric constant of the solvent surrounding the ion, ε_o the dielectric constant of the bulk solvent, a is the crystallographic radii of the ion. b-a is taken to be equal to the solvent radius. ε_1 was taken equal to 2 for all organic solvents, and

$$\Delta G_n^o = ma + c \qquad (17)$$

where m and c are constants characteristic of the solvent.

The free energy of transfer can be calculated from the relation [29].

$$\Delta G^{o}_{tr} = \Delta G^{o}_{s} - \Delta G^{o}_{h} \qquad (18)$$

ΔG^{o}_{h} is the free energy of hydration which is usually known experimentally and therefore, need not be calculated.

For ions hydrated in the organic phase with the first and second electrostatic layer being water [29].

$$\Delta G^{o}_{e} = \frac{N(ze)^2}{8\pi\varepsilon_o}\left\{\left(\frac{1}{\varepsilon_1}-1\right)\left(\frac{1}{a}-\frac{1}{b}\right)+\left(\frac{1}{\varepsilon_m}-1\right)\left(\frac{1}{b}-\frac{1}{c}\right)+\left(\frac{1}{\varepsilon_o}-1\right)\frac{1}{c}\right\}$$

ϵ_m is the dielectric constant in the second electrostatic layer (c-b) which is estimated from the Onsager equation. Other symbols have their usual meaning. Therefore, using ΔG^{o}_{e} and ΔG^{o}_{n} values we can calculate ΔG^{o}_{s} for the hydrated ion in the organic phase. The ΔG^{o}_{tr} values for ions hydrated in an organic phase are much more negative than for the unhydrated ions.

2.3 Ion Transfer

When the liquid-liquid interface is externally polarized ion transport takes place predominantly at the liquid-liquid interface because both liquids are ion permeable while electron transfer predominates at the solid-liquid interface because of

high electron conductivity of the solid electrode phase. At the liquid-liquid interface ion transfer can be classified into simple and facilitated ion transfer. Ion transfer can be facilitated by complexation, ion pair formation and precipitation.

2.3.1. Simple ion transfer

For a simple ion transfer across ITIES of the type,

$$i^{z}(w) \leftrightarrows i^{z}(o) \qquad (20)$$

and for a reversible diffusion controlled ion transfer the Galvani potential difference formed at the interface at equilibrium is given by Equation (6). That is,

$$\Delta_o^w \varphi_i = \Delta_o^w \varphi_i^\circ + \frac{RT}{z_i F} \ln \frac{a_i(o)}{a_i(w)}$$

Since $a = \gamma C$

$$\Delta_o^w \varphi_i = \Delta_o^w \varphi_i^\circ + \frac{RT}{z_i F} \ln \frac{\gamma_i(o)}{\gamma_i(w)} + \frac{RT}{z_i F} \ln \frac{C_i(o)}{C_i(w)}$$

where γ_i is the activity coefficient of the ion i.

The flux balance at the half-wave potential is given by

$$D_i^{1/2}(w)\ C_i(w) = D_i^{1/2}(o)\ C_i(o) \qquad (21)$$

and the half-wave potential becomes,

$$\Delta^{w}_{o}\varphi_{1/2i} = \Delta^{w}_{o}\varphi^{o}_{i} + \frac{RT}{2z_iF} \ln \frac{D_i(w)}{D_i(o)} + \frac{RT}{z_iF} \ln \frac{\gamma_i(o)}{\gamma_i(w)} \qquad (22)$$

2.3.2 Facilitated Ion Transfer

At the ITIES the potential at which an ion is transferred from one phase to the other is, in the case of simple ion transfer, dependent on the solvation properties of the ion in both phases. The presence of an ionophore further reduces the potential at which an ion is transferred; the magnitude of which reduction depends on the stability constant of the complex formed and/or ion association constant and, in the case of precipitate formation, on the solubility product of the precipitate. This phenomenon increases the scope of the ITIES by increasing the number of ion that can be investigated [1].

Let us consider the reaction

$$M^{z+}(w) + n\,L\,(o) \rightleftharpoons ML_n^{z+}\,(o) \qquad (23)$$

where M^{z+} is a metal ion with a charge z and L is the ionophore (ligand). Since charge the transfer reaction at the ITIES is generally reversible the potential difference between the aqueous and organic phase is given by,

$$\Delta_o^w\varphi = \Delta_o^w\varphi^o_{M^{z+}} + \frac{RT}{zF} \ln \frac{a_{M^{z+}}(o)}{a_{M^{z+}}(w)}$$

$$= \Delta_o^w\varphi^o_{ML_n^{z+}} + \frac{RT}{zF} \ln \frac{a_{ML_n^{z+}}(o)}{a_{ML_n^{z+}}(w)}$$

The complexation can take place either in the organic or in the aqueous phase. As to the site of the complex formation reaction, there is no universal agreement. Koryta [2] belies that the complex formation occurs in the organic phase after the transfer of the metal ion from the aqueous to the organic phase. The thermodynamically unfavorable transfer of the metal ion is compensated by its energetically favorable complexation, that is,

$$M^{z+}(w) \rightleftharpoons M^{z+}(o) \qquad (25)$$

$$M^{z+}(o) + nL\ (o) \rightleftharpoons ML_n^{z+}(o)$$

for which the Galvani potential difference is given by

$$\Delta_o^w\varphi = \Delta_o^w\varphi^o_{M^{z+}} + \frac{RT}{zF} \ln \frac{C_{ML_n^{z+}}(o)}{K_{ML_n^{z+}}(o)\ C_L^n(o)\ C_{M^{z+}}(w)}$$

$$+ \frac{RT}{zF} \ln \frac{\gamma_{M^{z+}}(o)}{\gamma_{M^{z+}}(w)} \qquad (26)$$

$$\text{Where } K_{ML_n^{z+}}(o) = \frac{C_{ML_n^{z+}}(o)}{C_{M^{z+}}(o)\ C_L^n(o)} \qquad (27)$$

Let us consider the simplest case in which the metal forms a complex with a single ligand

$$M^{z+}(w) + L(o) \rightleftharpoons ML^{z+}(o)$$

In most experimental investigations the concentration of the metal ion in the aqueous phase is taken in excess of the concentration of L in the organic phase, i.e.,

$$C_{M^{z+}}(w) \gg C_L(o) \qquad (28)$$

Hence only the diffusion of L and ML^{z+} in the organic phase need be considered. From the flux balance at the half-wave potential

$$D_{ML^{z+}}^{1/2}(o)\ C_{ML^{z+}}(o) = D_L^{1/2}(o)\ C_L(o) \qquad (29)$$

The half wave potential is then expressed as

$$\Delta_o^w\varphi_{1/2,ML^{z+}} = \Delta_o^w\varphi^{\theta}_{M^{z+}} + \frac{RT}{2zF}\ln\frac{D_L(o)}{D_{ML^{z+}}(o)} - \frac{RT}{zF}\ln K_{ML^{z+}}(o)\ C_{M^{z+}}(w) \qquad (30)$$

where $\Delta_o^w\varphi_H z+^{\theta}$ is the formal potential for ion transfer which includes the activity coefficient terms.

The value of the stability constant, $K_{HL}^{z+}(o)$ can be easily calculated from Eqn. (30) if we know, $\Delta_o^w\varphi_{HL}^{z+}$, assuming that $\gamma=1$ and $D_L=D_{HL}^{z+}$. We can also calculate the stability constant from the shift of half-wave potential of both the uncomplexed and complexed ion transfer. On the other hand Yoshida et al.[12] argued that the complexation occurs in the aqueous phase following the transport of the ionophore from the organic to the aqueous phase, even with ionophores (carriers) having low aqueous solubility, that is,

$$
\begin{array}{c}
L(o) \rightleftharpoons^{k_D} L(w) \\
nL(w) + M^{z+}(w) \rightleftharpoons ML_n^{z+}(w) \\
ML_n^{z+}(w) \rightleftharpoons ML_n^{z+}(o)
\end{array}
\qquad (31)
$$

The Galvani potential difference is given by

$$
\Delta_o^w\varphi = \Delta_o^w\varphi^{\circ}_{ML_n^{z+}} + \frac{RT}{zF} \ln \frac{a_{ML_n^{z+}}(o)}{a_{ML_n^{z+}}(w)} \qquad (32)
$$

Considering the formation of the monocomplex and for the condition $C_M^{z+} >> C_L$ the diffusion of M^{z+} in the aqueous phase need not be considered and at half-wave potential, the flux balance is given by,

$$
C_{ML}^{z+}(o)\ D_{ML^{z+}}^{1/2}(o) = C_L(o)\ D_L^{1/2}(o) \qquad (33)
$$

$$
\Delta_o^w\varphi_{1/2,ML^{z+}} = \Delta_o^w\varphi_{ML^{z+}} + \frac{RT}{zF} \ln K_D + \frac{RT}{2zF} \ln \frac{D_L(o)}{D_{ML^{z+}}(o)} + \frac{RT}{zF} \ln K_{ML^{z+}}(w)\ C_{M^{z+}}(w) \qquad (34)
$$

The transfer of an ion can also be facilitated by ion association. This is especially true in solvents of low dielectric permittivity where ion association is a common occurrence. When this ion association in the organic phase is taken into account, the expression for the half-wave potential, of ion i^z, takes the form:

$$\Delta_o^w\varphi_{1/2} = \Delta_o^w\varphi_i^o + \frac{RT}{z_iF} \ln \{D_i(w)^{1/2}/(D_i^{1/2}(o) + a_c(w) K_a D_{ic}^{1/2}(o))\}$$
$$- \frac{RT}{zF} \ln \{ (\gamma_i(o) + \gamma_{ic}(o))/\gamma_i(w)\} \qquad (35)$$

$a_c(w)$ is the activity of the anion or the cation of the supporting electrolyte in the organic phase, K_a the ion association constant of the transferred ion with the respective ion of the supporting electrolyte. The subscript ic indicates ion associate. For the facilitated transfer of an ion based on precipitate formation, i.e.,

$$M^+(w) + X^-(o) \rightleftharpoons MX\ (o) \downarrow \qquad (36)$$

the standard Gibbs energy of transfer is given by,

$$\Delta G_{tr,MX} = \Delta G_{tr,M^+} + \Delta G_{tr,X^-}$$
$$= RT \ln \frac{K_{sp}(w)}{K_{sp}(o)} \qquad (37)$$

where K_{sp} is the solubility product constant.
Accumulation of the precipitate at the interface can hinder ion transfer [109].

3. ELECTROCHEMICAL METHODS

The interface between two immiscible electrolyte solutions has been investigated using electrochemical methods. There has been a surge of electrochemical methods especially after Koryta [2] described the analogy between metal/solution and liquid-liquid interfaces and after Samec [39] introduced the four electrode potentiostat with IR drop compensation, which took over for all potential controlled experiments. The potentiostat consists of two reference electrodes which serve to control or measure the potential of the system and two counter electrodes which serve as a source and sink of current.

3.1 Cyclic Voltammetry

Cyclic voltammetry is one of the most commonly used electrochemical method for the analysis of kinetic and thermodynamic parameters. In dc cyclic voltammetry [110] a triangular dc voltage is applied to the electrochemical cell and the current response is recorded as a function of the applied voltage.

At the ITIES, charge transfer is usually very fast and the process is reversible and diffusion controlled for which the current is given by the Randels-Servick equation

$$i = z^{2/3}FAC_i^{o}D_i^{1/2}\nu^{1/2}(F/RT)^{1/2}\pi^{1/2}\chi_{(at)} \qquad (38)$$

i is the current (Ampere), A, area of the interface (cm^2), D,the diffusion coefficient (cm^2sec^{-1}), ν, polarization rate (volt sec^{-1}), C_i^{o}, bulk concentration of the ion i (mole dm^{-3}), $\chi(at)$,the current function tabulated by Nicolson & Shain [110] and, the peak potential ($\Delta_o^{w}\varphi_p$) is related to the half wave potential by,

$$\Delta_o^{w}\varphi_{p,i} = \Delta_o^{w}\varphi_{1/2,i} - 1.09\,\frac{RT}{zF} \qquad (39)$$

or, at 298k ,

$$\Delta_o^{w}\varphi_{p,i} = \Delta_o^{w}\varphi_{1/2,i} \pm \frac{0.0285}{|z|} \qquad (40)$$

where - and + stands for the negative and positive currents respectively.

Some of the diagnostic criteria for the reversibility of ion transfer are: the dependence of i_p on $v^{1/2}$ should be linear, the peak to peak separation should be given by $60/|z|$ in mv where z= charge of the ion, the ratio of the anodic and cathodic peak currents should be equal to one, i.e.,

$$i_{p,a}/i_{p,c} = 1$$

The dc cyclic voltammetric technique has been extended to the ac mode by superimposing an ac voltage on the dc triangular ramp [111, 112]. Either the fundamental or second harmonic ac response is recorded as a function of the applied dc potential. AC cyclic

voltammerty has a considerable advantage over the dc mode because of its better response (improved wave shape, which makes evaluation of $\Delta_o^w\varphi_{\frac{1}{2}}$ easy, and discrimination against charging current, which brings about better sensitivity). For a reversible charge transfer the forward and reverse scans overlap with **half-peak width of 90/|z| (z is charge on the ion).**

3.2 Flow Analysis

At the ITIES flow analysis can be done either using concentration step (changing the flow of the carrier solution to the carrier solution containing the ion to be studied) or concentration pulse (injecting a small amount of the ion into the carrier stream). In the wall-jet arrangement , a jet of solution issues from a circular nozzle and impinges perpendicularly at the detector. The counter electrode is placed remote from the wall-jet.
The General equation for mass transfer is given by [113]

$$\frac{\partial c}{\partial t} = D\left(\frac{\partial^2 c}{\partial x^2} + \frac{\partial^2 c}{\partial y^2} + \frac{\partial^2 c}{\partial z^2}\right) - \left(V_x \frac{\partial c}{\partial x} + V_y \frac{\partial c}{\partial y} + V_z \frac{\partial c}{\partial z}\right) \qquad (41)$$

where c is the concentration (c (x,y,z,t)), V_x,V_y,V_z are component of the velocity in the x,y, and z direction respectively. The first term on the right hand side of Eqn. (41) is the rate of change of concentration resulting from diffusion and the second term is the rate of change of concentration due to convection.

Since the mathematics is very difficult it is only in a few cases that complete solution can be derived by introducing the appropriate boundary conditions.

In the wall-jet arrangement when a solution flows over the hydrophilic membrane a very thin layer is formed adjacent to the surface (hydrodynamic boundary layer) in which the velocity gradient normal to the surface is very large.

According to Gunasingham and Fleet [114] the boundary layer thickness is given by

$$\delta_{bl} = 5.8\ \pi^{3/4}\ a^{1/2} \upsilon^{3/4} X^{5/4} V^{-3/4} \qquad (42)$$

where a is the diameter of the nozzle; υ, the kinematic viscocity; V, the flow rate.

Within the boundary layer there exists a diffusion layer, adjacent to the membrane. The average thickness of this diffusion layer is given by [114],

$$\delta_{dl} = 2.80 D_w^{1/3}\ a^{1/2}\ \upsilon^{5/12}\ R^{5/4}\ V^{-3/4} \qquad (43)$$

where R is the radius of the detector, and D_w, the diffusion coefficient of the ion in the aqueous phase.

At the membrane stabilized interface, the current relation was d derived theoretically for the flow injection system [115].

consider the figure below

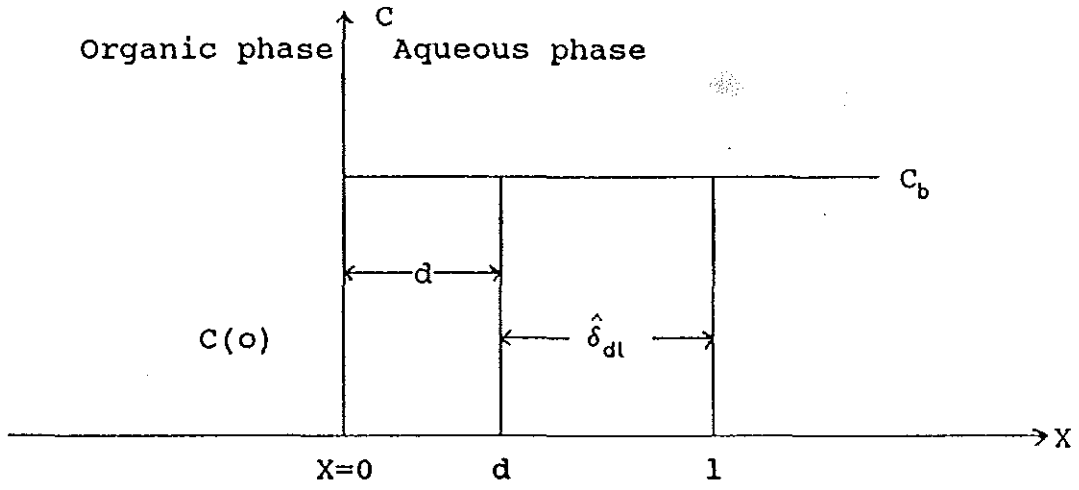

Fig. 1. The Diffusion Layer .

The water /oil interface is supposed to be at x=0, the membrane extends to x=d and the steady state diffusion layer, δ_{dl} , extends from x=d to x=1. In order to get an operational solution of the convective transport Hundhammer et al. [115] assumed linear diffusion within the membrane and the region attributed to $\hat{\delta}_{dl}$.

Using the boundary conditions

$$t = 0 \quad c = o \qquad -\infty < x < d$$

$$c = c_b \qquad x \geq d$$

$$t > o$$

$$c(t) = c_b - s_{tp}\,(t)\,c_b \qquad x \geq l$$

$$c = o \qquad x \to -\infty$$

$$\frac{c_o \gamma_o}{c_w \gamma_w} = \exp\left(ZF(\Delta_o^w\varphi - \Delta_o^w\varphi^o)\,/RT\right) = o\,, \quad x = o$$

$$c_w = c_M \qquad x = d$$

and *the flux balance*

$$D_o\,(\frac{\partial c_o}{\partial x}) = D_m\,(\frac{\partial c_m}{\partial x}) \qquad x = o$$

$$D_m\,(\frac{\partial c_m}{\partial x}) = D_w\,(\frac{\partial c_m}{\partial x}) \qquad x = d$$

where $S_{tp}(t)$ is the unit step function defined as

$$S_{tp}\,(t) = o \qquad for \qquad o \leq t \leq t_p$$

and

$$S_{tp}\,(t) = 1 \qquad for \qquad t > t_p$$

and t_p is the length of the concentration pulse acting on the sensor, and finally introducing the effective diffusion coefficient.

$$D = 1\,/\,(\delta_{dl}\,/\,D_w + d\,/\,D_m)$$

They showed that

$$\ln\ (t^{1/2}\ i)\ =\ \ln\ \{zFAC^{\circ}(\frac{D}{\pi^{1/2}}\}\ -\frac{D^2}{4Dt} \qquad (44)$$

The steady state current according to [115] is given by

$$i_{ss}\ =\ (zFAC^{\circ}D)/l \qquad (45)$$

The steady state current is more convenient for the evaluation of the effective diffusion coefficient.

4. EXPERIMENTAL

The electrolytic cell employed consisted of a Ag/AgCl/Cl^- (sat'd KCl) reference electrode immersed in 10 mM $MgSO_4$ aqueous solution and the second reference electrode, also Ag/Agcl/Cl^-(sat'd KCl), was connected to the nitrobenzene phase by means of a Luggin capillary inside which a water (Sat'd KCl) /nitrobenzene (CVTPB) interface was formed.

The base electrolyte for the aqueous phase was 10 mM $MgSO_4$ and 10 mM CVTPB for the organic phase. Twice distilled and deionized water was used throughout the experiment.

All chemicals were reagent grade (except $MgSO_4$ which was GP grade) and were used without further purification.
Stock solutions of 10mM $NiSO_4$, 10 mM $CdSO_4$, and 10mM $FeSO_4$ were prepared and used by dilution as required. The $Ni(bipy)_3^{2+}$ complex was prepared by mixing $NiSO_4$ and bipyridine in 1:3 mole ratio in water.

For the study of facilitated transfer, 10 mM 2,2'-bipyridine was prepared in nitrobenzene containing 10 mM CVTPB. Nitrobenzene (BDH) was purified by washing first three times with 0.1N H_2SO_4 followed by 0.1N KOH for neutralization; finally it was washed with distilled water until it become neutral. The washed

nitrobenzene was distilled under reduced pressure and only the middle of the distillate was collected and stored for use. CVTPB was prepared by mixing NaTPB and CVCl in methanol and the precipitated CVTPB was filtered off and washed with distilled water until it was free from Cl^-. m.pt 114-115 °c.

The membrane used was the hydrophilic dialysis membrane PT-150 or PT-325. A disk of 1.5 cm in diameter was cut and immersed in 10 mM aqueous solution for half an hour. The thickness of the dry and swollen membranes were (10 ± 3) and (20 ± 3) μm for PT-150 and (20 ± 1 & 41 ± 1) μm for PT-325.

The swollen membrane was mounted on a PTFE membrane holder using an o-ring and tightly screwed in place. After filling the inner compartment with the organic phase, the membrane was dipped into the aqueous phase. Fig. 2 depicts the cell arrangement for the flow analysis with the wall-jet arrangement. In the organic phase Pt wire was used as a counter electrode while the counter electrode in the aqueous phase was stainless steel which also served as the jet inlet. This was properly placed so that the solution impinged perpendicularly and uniformly at the membrane, or the working interface, which had an area of 0.25 cm^2. For voltammetric experiments under stationary conditions a Pt counter electrode was used in the aqueous phase. A block diagram of the system used for flow injection analysis is shown in Fig. 3. The carrier solution, which at the same time served as a supporting

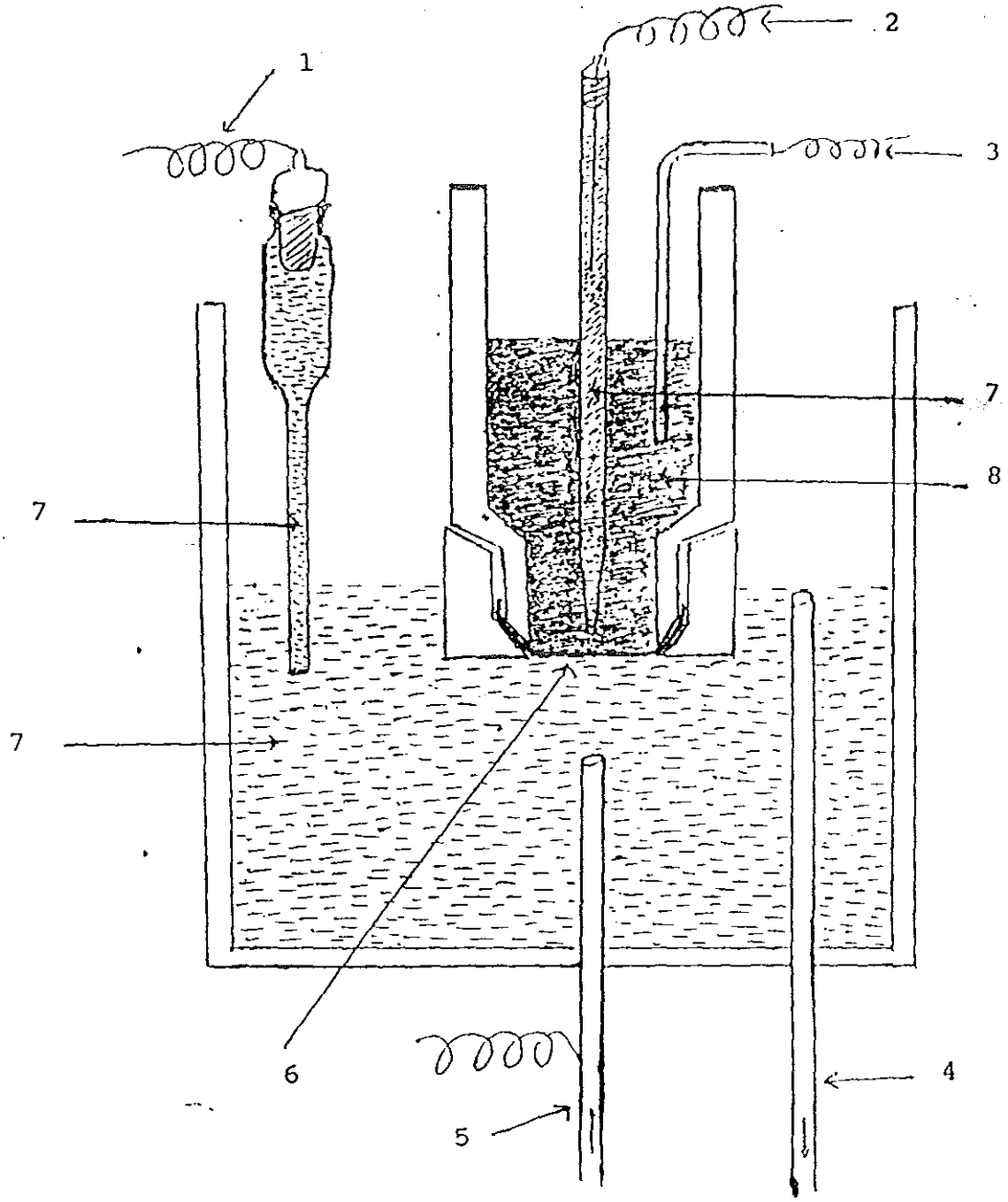

Fig. 2 Wall-jet electrochemical cell

1, aqueous reference electrode; 2, organic reference electrode; 3, organic counter38lectrode; 4, outlet; 5, jet inlet which at the same time serves as the aqueous counter electrode; 6, membrane; 7, aqueous phase; 8, organic phase.

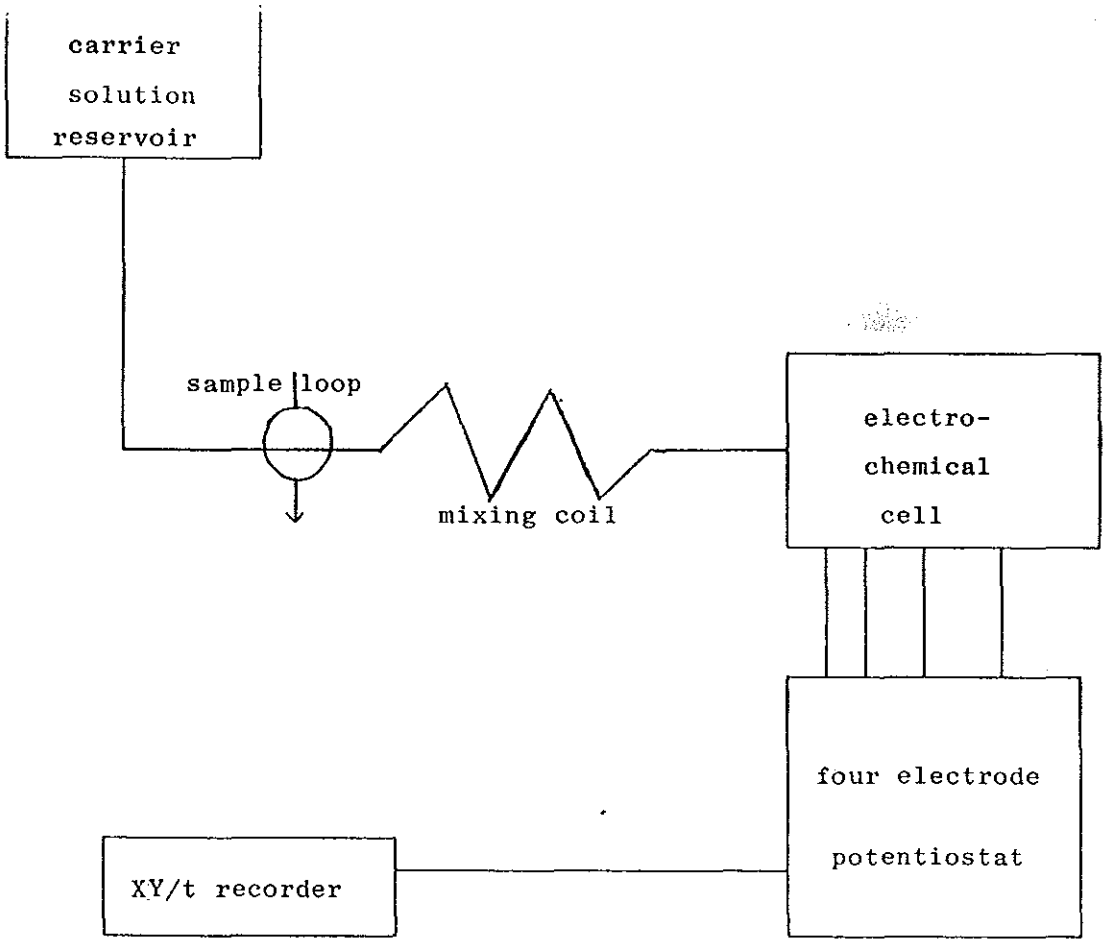

Fig. 3 Block diagram for the system flow injection analysis.

electrolyte, was positioned at a height of 1/2 meter and the flow rate was controlled by gravity. The solution of the ion to be investigated was injected in to the carrier stream with a sample loop of 25μl capacity. For the continuous flow analysis two aspirator bottles, one filled with the carrier solution and anther filled with the carrier solution containing the ion to be investigated, were positioned at the same height. The flow of the carrier solution was changed into the carrier solution containing the ion under investigation using a three way stopcock. All tubing was made of polyethylene. The w/nb interface was polarized using a signal generator(MP1052 Electroanalyzer, Mckee Pederson Inst.), through a home made four electrode potentiostatic circuit with a feed back loop for IR compensation.

The 5mv peak-to-peak sinusoidal voltage, which was superimposed on the triangular voltage, in the ac cyclic experiment, was generated by a Tektronix FG-501 frequency generator. In the ac experiments, the potentiostatic current output was fed to a PAR model 5204 lock-in analyzer and the inphase component of the current was recorded against the applied dc potential. The block diagram of the electronic arrangement for the ac cyclic voltammetry experiment is shown in Fig. 4. In the dc cyclic voltammetric experiment the current output of the potentiostat was directly connected to the x-y recorder.

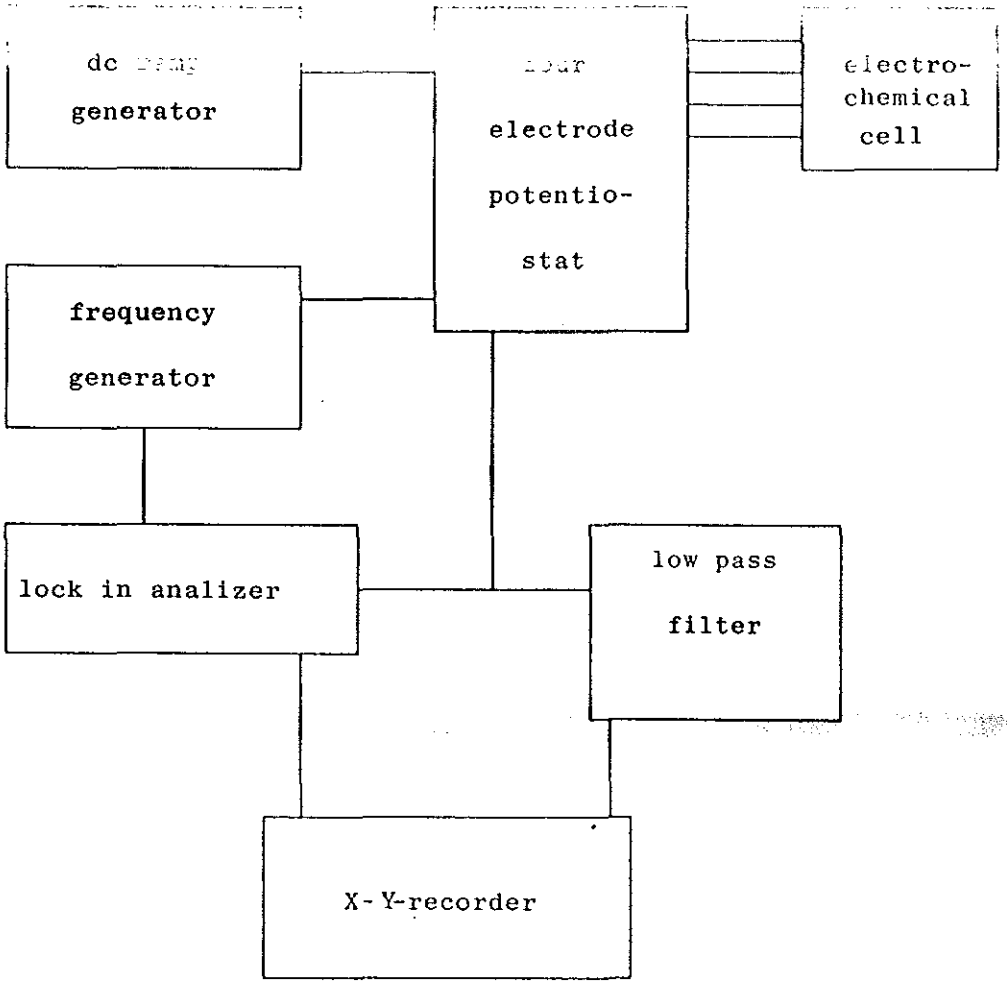

Fig. 4 Block diagram of the electronic set up for the ac cyclic voltammetry experiment

The basic cell arrangement used in all the experiments was:

Ag/AgCl/KCl (sat'd)/CVTPB/membrane/ 10mM $MgSO_4$/AgCl/Ag

All experiments were done at a laboratory temperature of 21±3°c.

5. RESULTS and DISCUSSION

Throughout the study 10 mM $MgSO_4$ was used as a supporting electrolyte in the aqueous phase while 100, 10 or 0.1 mM CVTPB was used in the organic phase (nitrobenzene). The potential window was limited by the transfer of Mg^{2+} and/or TPB^- in the higher potential region and SO_4^{2-} and/or CV+ in the lower potential region. The potential window was about 500 mv. Fig. 5 shows the dc and ac cyclic Voltammograms for the base electrolytes. When 10 mM 2, 2'-bipyridine was present in the organic phase no facilitated proton transfer was observed up to pH 5. However, when the pH was lowered to 4.5 the facilitated transfer of H^+ was noticeable. Since the pH of investigated transition metal ion solutions and that of the carrier solution was 6, H^+ transfer could not occur.

5.1. Flow Injection

In the flow injection analysis 25 μl of the ion to be studied was injected into the carrier stream (supporting electrolyte). The injected sample forms a zone which is then transported towards the voltammetric sensor, i.e., ITIES where the facilitated transfer of the metal ion occurs. The magnitude and shape of the observed peak is dependent on the kinetics and thermodynamics of the complex formation as well as on the transport processes.

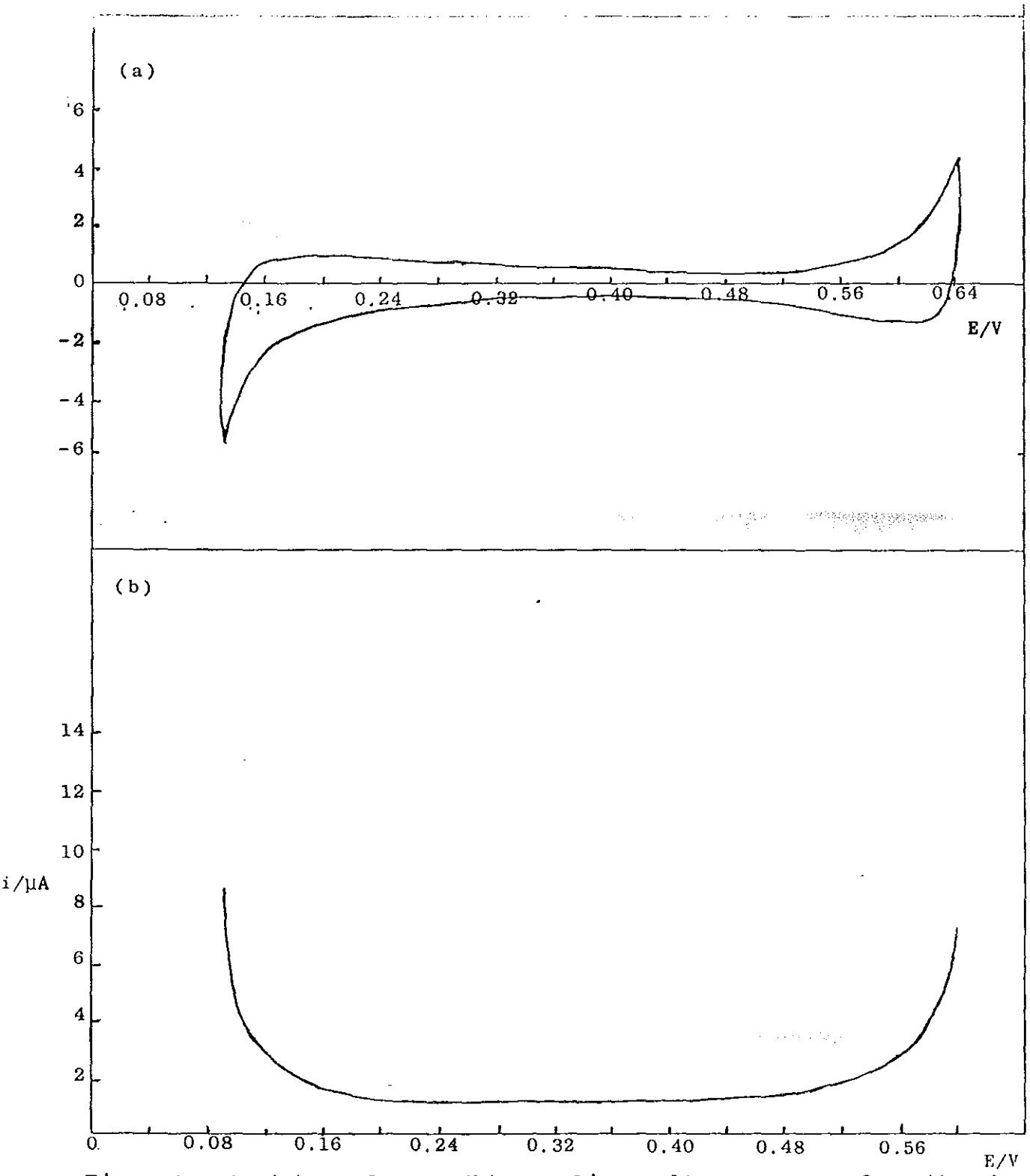

Fig. 5 DC (a) and AC (b) cyclic voltammograms for the base electrolytes. Aqueous phase 10 mM MgSO4, organic phase 10 mM CVTPB in nitrobenzene.

5.1.1. I-V Characteristics

The dependence of current peak height on the applied potential (E_{app}.) was studied for the facilitated transfer of Fe^{2+}, Cd^{2+} and Ni^{2+} and complex ion transfer of Ni $(bipy)_3^{2+}$. Tables 1 and 2 show the values of i_p for different applied potentials.

The plot of current peak height versus the applied potential for the transfer Fe^{2+} facilitated by 2, 2'-bipyridine in the organic phase is shown in Fig. 6. An S-shaped curve with a half wave potential, the most important qualitative feature of the curve, of 275 mV was obtained. Quantitative analysis of the transferring metal ion is also possible from the dependence of the current peak height on its concentration at a constant potential in the limiting current region [9].

The transfer of Cd^{2+} facilitated by 2, 2'-bipyridine is plotted in Fig. 7 and has similar features to that of Fe^{2+}, with a half wave potential of 310 mV.

Table 1 Dependence of i_p on the applied potential for the facilitated transfer of iron (II). (0.1 mM $FeSO_4$ aqueous phase and 10 mM 2, 2'-bipyridine with 10 mM CVTPB in nitrobenzene).

E/ mV	$i_p/10^{-7}$ Ampere
175	0.25
200	0.30
225	0.70
250	2.0
275	5.65
300	7.6
325	8.5
350	9.2
375	9.3

Table 2 Dependence of i_p on the applied potential for the facilitated transfer of Cadmium (II). (1 mM $CdSO_4$ aqueous phase and 10 mM 2, 2'-bipyridine with 10 mM CVTPB in nitrobenzene).

E/mV	$i_p/10^{-7}$ Ampere
175	0.1
200	0.2
225	0.3
250	0.4
275	0.8
300	2.0
310	3.2
320	4.5
330	6.3
340	6.4

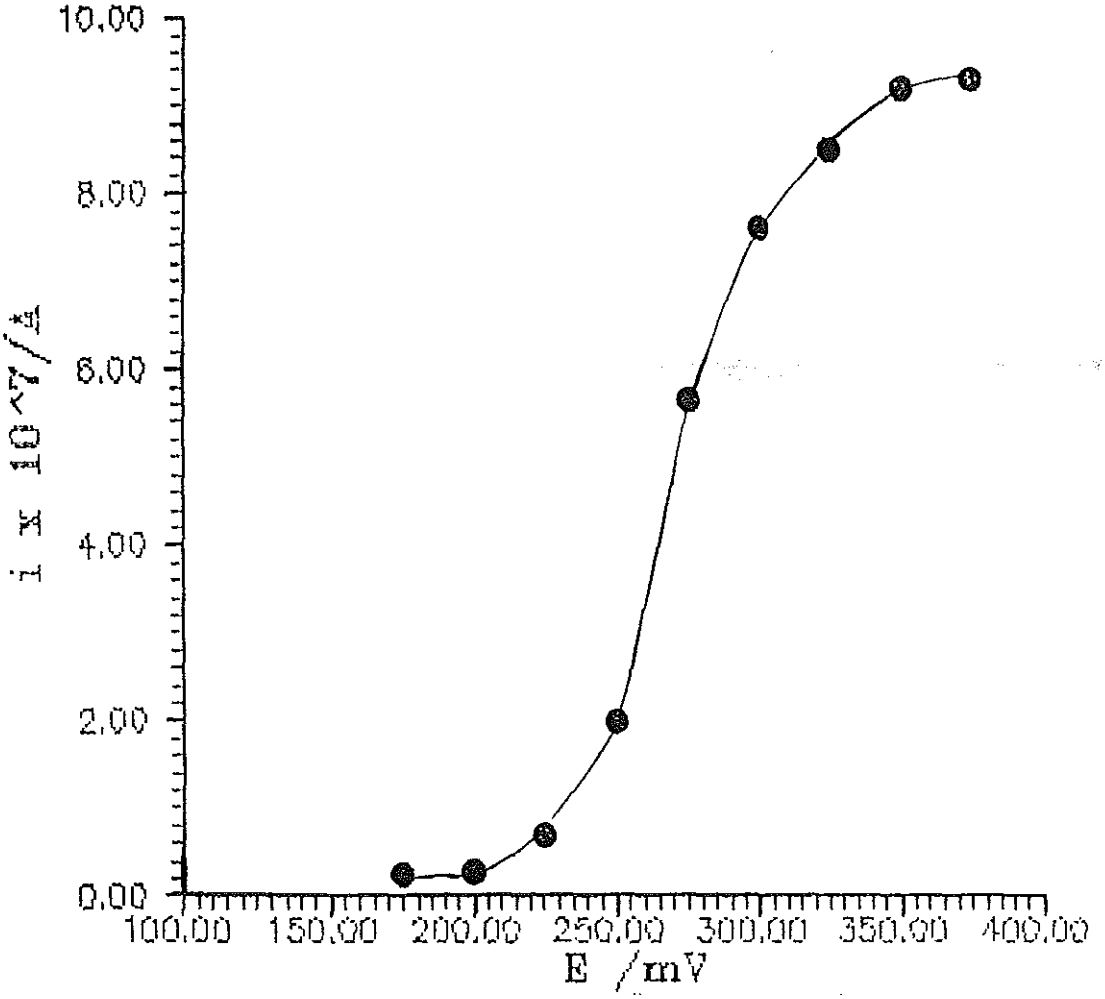

Fig. 6 Dependence of current peak height on the applied potential difference. Carrier stream 10mM MgSO4. Injected sample, 25 μl of 1.0 mM FeSO4 in 10mM MgSO4. Organic phase 10 mM 2,2' dipyridine + 10mM CVTPB in nitrobenzene.

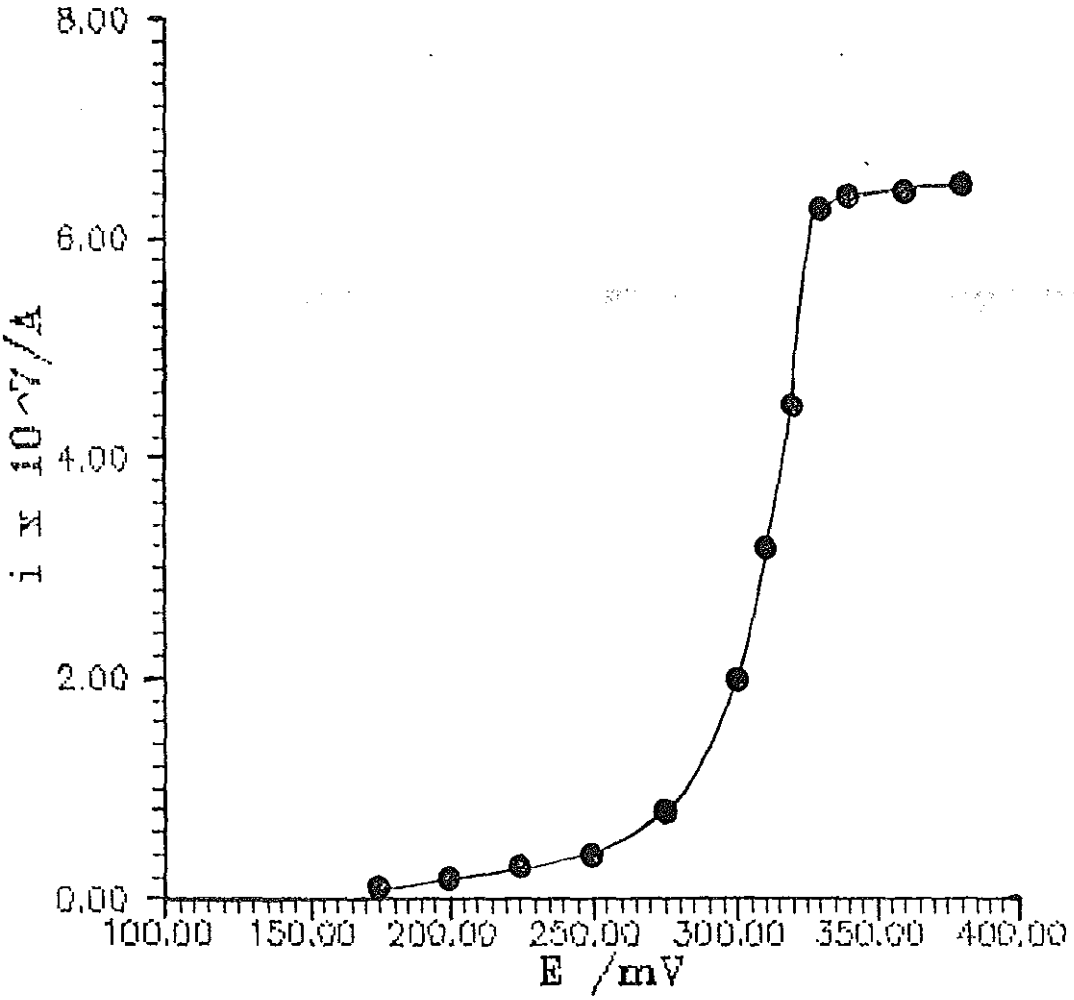

Fig. 7 Dependence of current peak height on the applied potential difference. Carrier stream 10 mM MgSO4. Injected sample 25μl of 1.0 mM CdSO4 in 10mM MgSO4. Organic phase 10 mM 2,2' dipyridine + 10mM CVTPB in nitrobenzene.

Table 3 and 4 shows the values of i_p for different applied potentials for Ni $(bipy)_3^{2+}$ and Ni^{2+}. An attempt to study the facilitated transfer of Ni^{2+} using 2, 2'-bipyridine in the organic

phase resulted in very poor I-V characteristics with a hardly discernible half-wave potential (Fig. 8a). On the other hand the transfer of Ni $(bipy)^{2+}_n$ showed an S shaped curve with a half wave-potential of 265 mV (Fig. 8b). Based on the magnitude of the successive stability constants (Table 5) we can assume that the complex investigated is the tris complex. This was further confirmed by the findings of Homolka and Wendt [96]. These authors, in their studies of multi-complexed ion transfer of Ni^{2+} with 2, 2'-bipyridine using 1:3 Ni^{2+} to 2,2'-bipyridine mole ratio observed the transfer of the tris complex only.

The experimentally obtained half-wave potentials for Fe^{2+}, Cd^{2+} and Ni $(bipy)_3^{2+}$ are nearly similar. Thus the assumption that in all cases the tris complex is transferred seems to be justified in view of the fact that the charge and size of the complex ions are very similar. The peak potential for the transfer of Cd^{2+} appeared at a more positive potential by about 40 mV. If it were due to the transfer of the bis complex it would be expected to appear at a more positive potential by at least 170 mV than that of the tris complex [14,96].

Table 3. Dependence of peak current i_p on the applied potential (E_{app}) for the complex ion transfer of $Ni(bipy)_3^{2+}$ (0.1 mM $Ni(bipy)_3^{2+}$ in 10mM $MgSO_4$ aqueous phase and 10 mM CVTPB in nitrobenzene).

E/mV	$i_p/10^{-7}$Ampere
175	0.1
200	**0.2**
225	0.5
250	1.2
275	**4.1**
300	5.2
325	5.3
350	5.4
375	5.4

Table 4. Dependence of peak current (i_p) on the applied potential (E_{app}) for the facilitated transfer of Ni^{2+}. (1 mM $NiSO_4$ in 10 mM $MgSO_4$ aqueous phase and 10 mM 2, 2' bipyridine with 10 mM CVTPB in nitrobenzene).

E/mV	$i_p/10^{-7}$Ampere
225	0.10
250	0.25
275	0.50
300	0.60
325	0.70
350	1.10
375	1.20
400	**1.30**
425	1.50
450	1.50
475	1.80
500	2.00

Since the replacement of two water molecules by one bipyridine molecule from the respective hydrated transition metal ions change the standard Gibbs energy of transfer of the complex by 170 mv or more. Therefore, the wave for Cd^{2+} transfer is ascribed to the transfer of the tris complex. The appearance of the peak at a more positive potential could be due to the much lower stability constant of the tris Cd^{2+} complex (Table 5).

Table 5: Successive Stability Constants for the Complexes of Fe^{2+}, Ni^{2+} and Cd^{2+} with 2,2'-bipyridine [116].

Ion	Fe^{2+}	Ni^{2+}	Cd^{2+}
log k_1	4.3	7.1	4.3
log k_2	3.7	6.8	3.5
log k_3	9.5	6.2	2.6

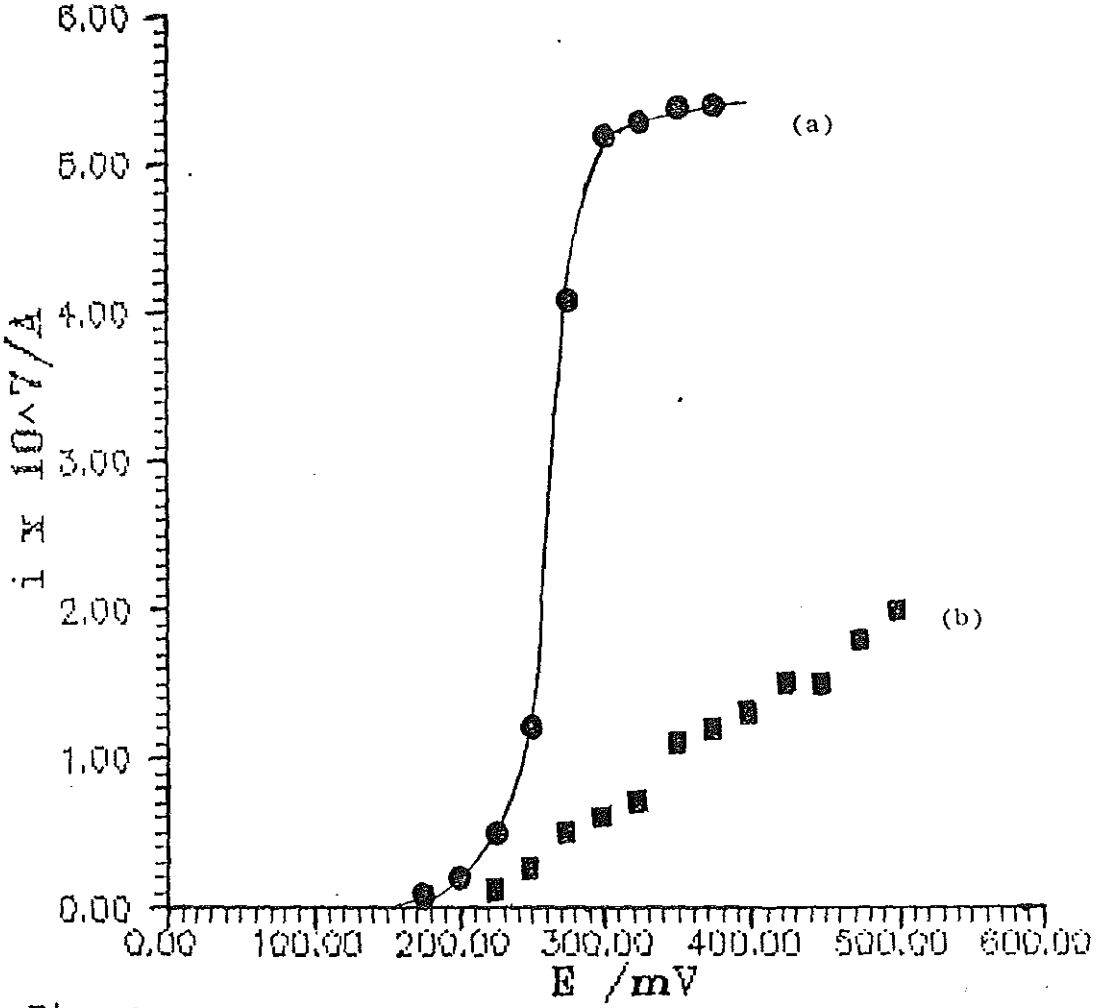

Fig. 8 Dependence of current peak height on the applied potential difference. Carrier stream 10 mM $MgSO_4$. (a) Complex ion transfer of $Ni(bipy)_3^{2+}$ (b) facilitated transfer of 1 mM Ni^{2+}. Organic phase 2, 2'-bipyridine + 10 mM CVTPB in nitrobenzene.

5.2. Kinetic and Thermodynamic Behavior

The thermodynamic and kinetic behaviour was studied by the analysis of the current-time response to an injected sample of the respective ion and by ac and dc voltammetry.

Figures 9 and 12 show the current-time response to an injected sample of 25 μl 10 mM Ni^{2+} and Fe^{2+}, Cd^{2+} and perchlorate ion at a potential within the limiting current region (320 mV). The current-time behavior for the transfer of Ni^{2+} shows a very broad peak indicating that there might be kinetic control by slow formation of the complex. The same behavior was observed in the complexation reaction rate study of the Ni^{2+} with 2,2'-bipyridine in aqueous solution [117], which was found to be more than 1000 times slower than that of Fe^{2+} and Cd^{2+}. For monodentate ligand substitution reaction of the divalent aquometal ion the rate of substitution is in most cases determined by the outer-sphere association constant and the water exchange rate of the outer-sphere complex as affected by charge and size of the metal ion and crysalfield stabilization energy . The rate determining step is usually the the first coordinate bond formation of the ligand. For multidentate ligand substitution reaction, depending on the nature of the multidentate ligand and metal ion the rate determining step can shift from the first coordination reaction to some later chelation step. Steric effects may become important in ring closure reactions as well as in the initial coordination step

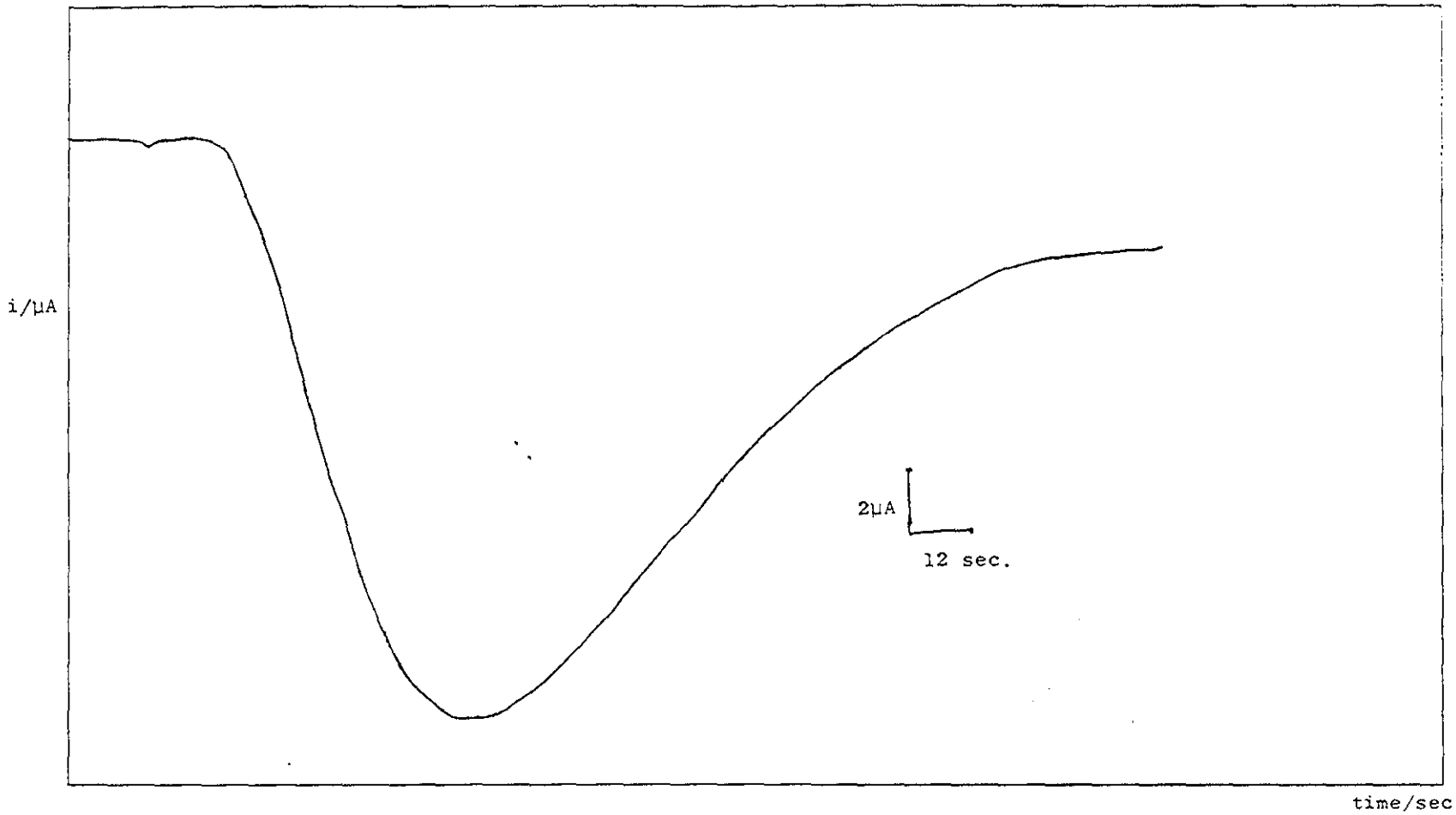

Fig. 9 Current time behaviour for the facilitated transfer of Ni(II). Carrier stream 10mM MgSO4. Injected sample 25 μl 10 mM NiSO4. Organic phase 10 mM 2,2'-bipyridine + 10mM CVTPB in nitrobenzene.

[119, 120]. For Ni^{2+}, Fe^{2+} and Cd^{2+} the rate of substitution reaction of the aquometal ion with 2,2'-bipyridine follows the order [117]

$$Ni^{2+} < Fe^{2+} < Cd^{2+}$$

This reactivity sequence parallels that observed for the water exchange rate for the metal ion [117]. The poor I-V curve for Ni^{2+} (Fig 8a) is also indicative of the slow kinetics of the complexation. Furthermore, the kinetically controlled transfer of Ni^{2+} was studied using ac cyclic voltammetry. In the ac voltammogram the forward and reverse scan did not overlap and different peak potentials were observed. For a reversible transfer at least the forward and reverse peaks should have the same E_p values. Ac cyclic voltammogram was run at different frequencies (Fig. 10). The plot of i_p Vs $\omega^{1/2}$ (Fig. 11) shows a linear dependence. For a reversible transfer a linear dependence of i_p on the square root of the frequency is expected.

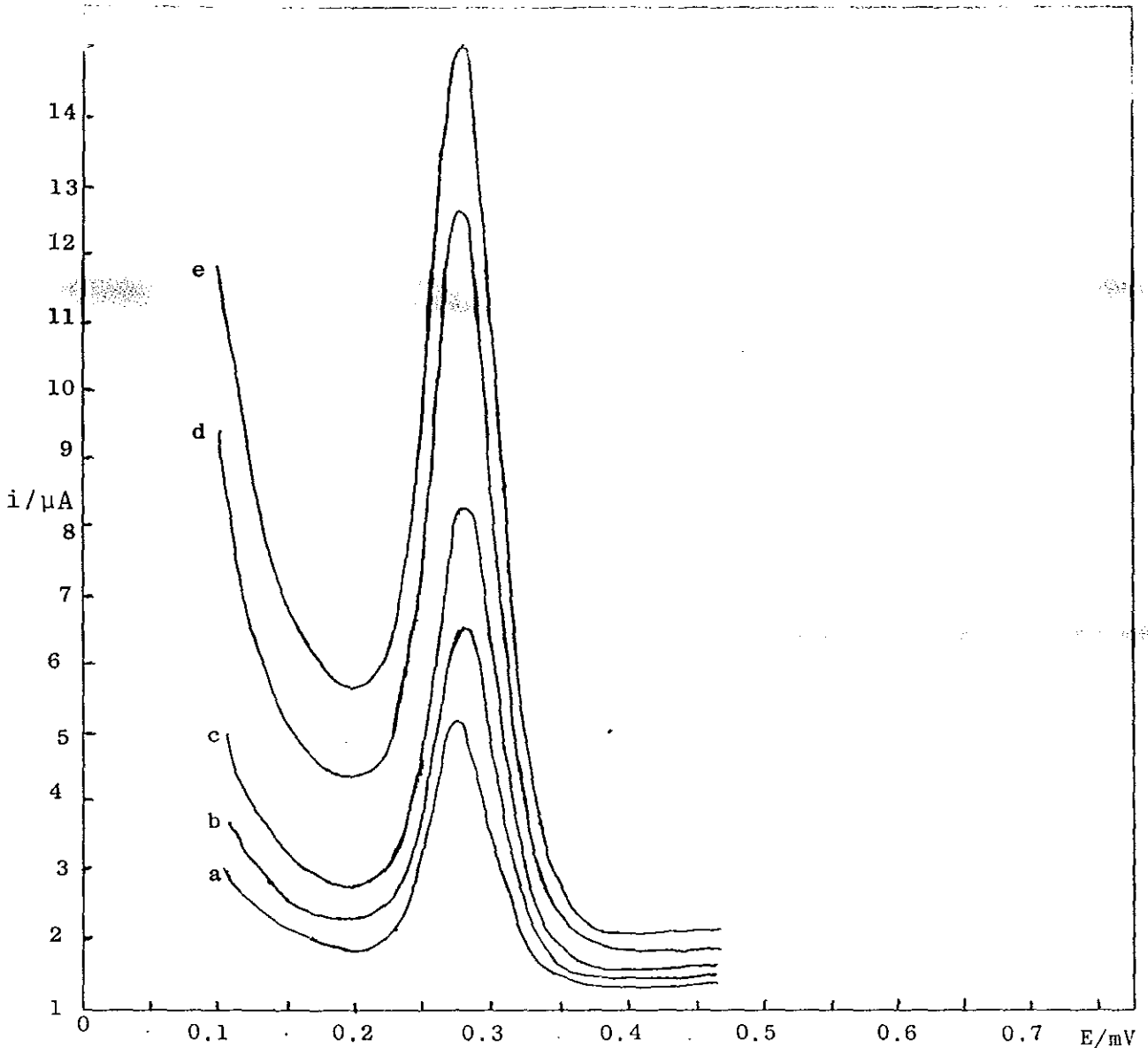

Fig. 10 AC cyclic voltammogram for the facilitated transfer of Ni(II) at different frequencies (a) 10 Hz (b) 15 Hz (c) 20 Hz (d) 30 Hz (e) 35 Hz. Sweep rate 12 mv/sec. Aqueous phase 10 mM NiSO4 in 10 mM MgSO4. Organic phase 10 mM 2,2'-dipyridine + 10 mM CVTPB in nitrobenzene.

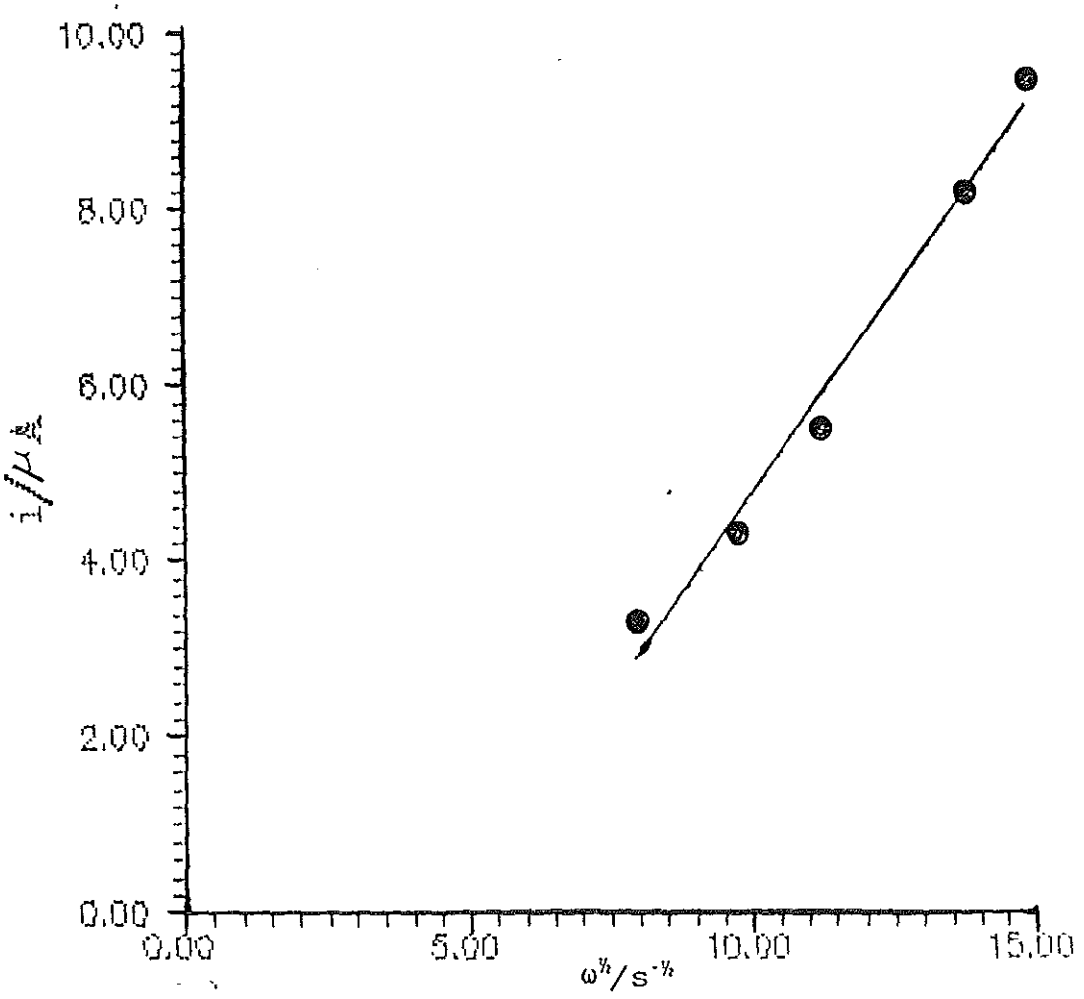

Fig. 11. Dependence of current peak height on the squareroot o frequency ($\omega^{1/2}$). (The facilitated transfer of 10 mM Ni(II) in 10 m MgSO4 aqueous phase and 10 mM 2,2'- bipyridine + 10mM CVTPB i nitrobenzene.)

On the other hand the facilitated transfer of Cd^{2+} and Fe^{2+} showed different behavior from that of Ni^{2+}. The i-t curves [Fig. 12], with fairly sharp peaks, indicate that the transfer of these ions is not kinetically controlled. The peaks for these ions have similar shape to that of perchlorate which is known to be diffusion controlled. The diffusion controlled reversible transfer of Cd^{2+} and Fe^{2+} can easily be inferred from the overlapping forward and reverse ac peaks and the half peak width (≈45mv).

Ac cyclic voltammograms for 10mM Fe^{2+} and Ni^{2+} in the aqueous and 10mM 2,2- dipyridyl in the nitrobenzene phase is shown in Fig. 13 and Fig 14. In both voltammograms two peaks are observed one at 280 mv and the other at 485 mv. The ac cyclic voltammogram for the complexed ion transfer showed one peak only at a potential very close to the peak at 280 mv. Therefore, it can be concluded that the peak at lower potential (280 mv) is due to the tris complex while the second peak at higher potential could be due to the bis complex of the metal ions. A similar result was obtained for the transfer of Cd^{2+} (Fig. 15). The relative stability constants for Fe^{2+} and Cd^{2+} can be deduced from the magnitude of their current peak heights. Based on this the relative stability of Fe^{2+}-bipy complex was found to be higher than that of the bis complex. This is in agreement with the stability constant of the complexes in aqueous phase (Table 5). The relative stabilities of

the successive complexes for Cd^{2+} deduced was not in agreement with the literature data (Table 5).

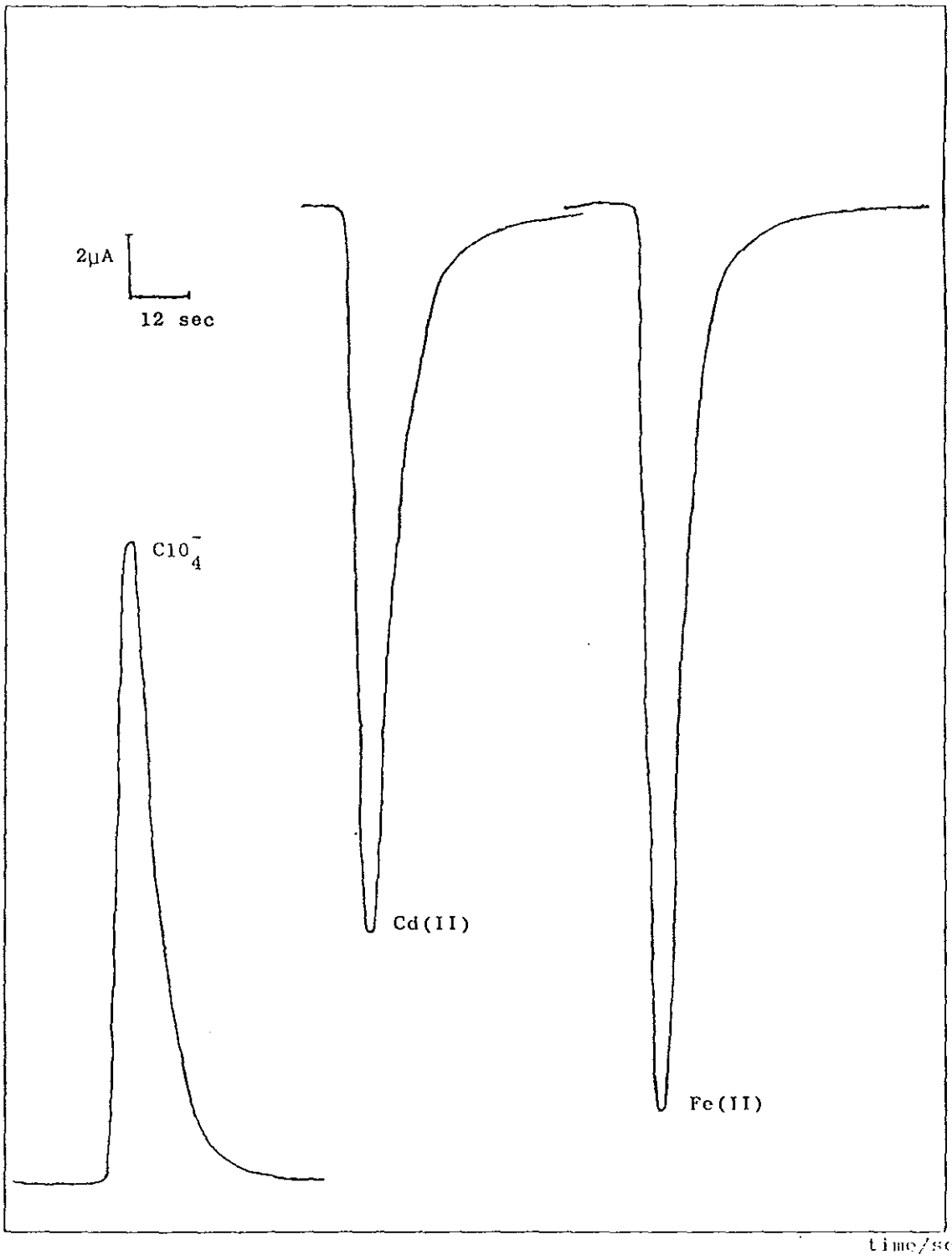

Fig. 12 Current-time behaviour for the facilitated transfer of Cd(II) and Fe(II). ClO_4^- is used as a reference. Carrier stream 10 mM MgSo4 in to which 25 μl of 10 mM CdSO4 and FeSO4 was injected. Organic phase 10 mM 2,2'-bipyridine + 10mM CVTPB in nitrobenzene.

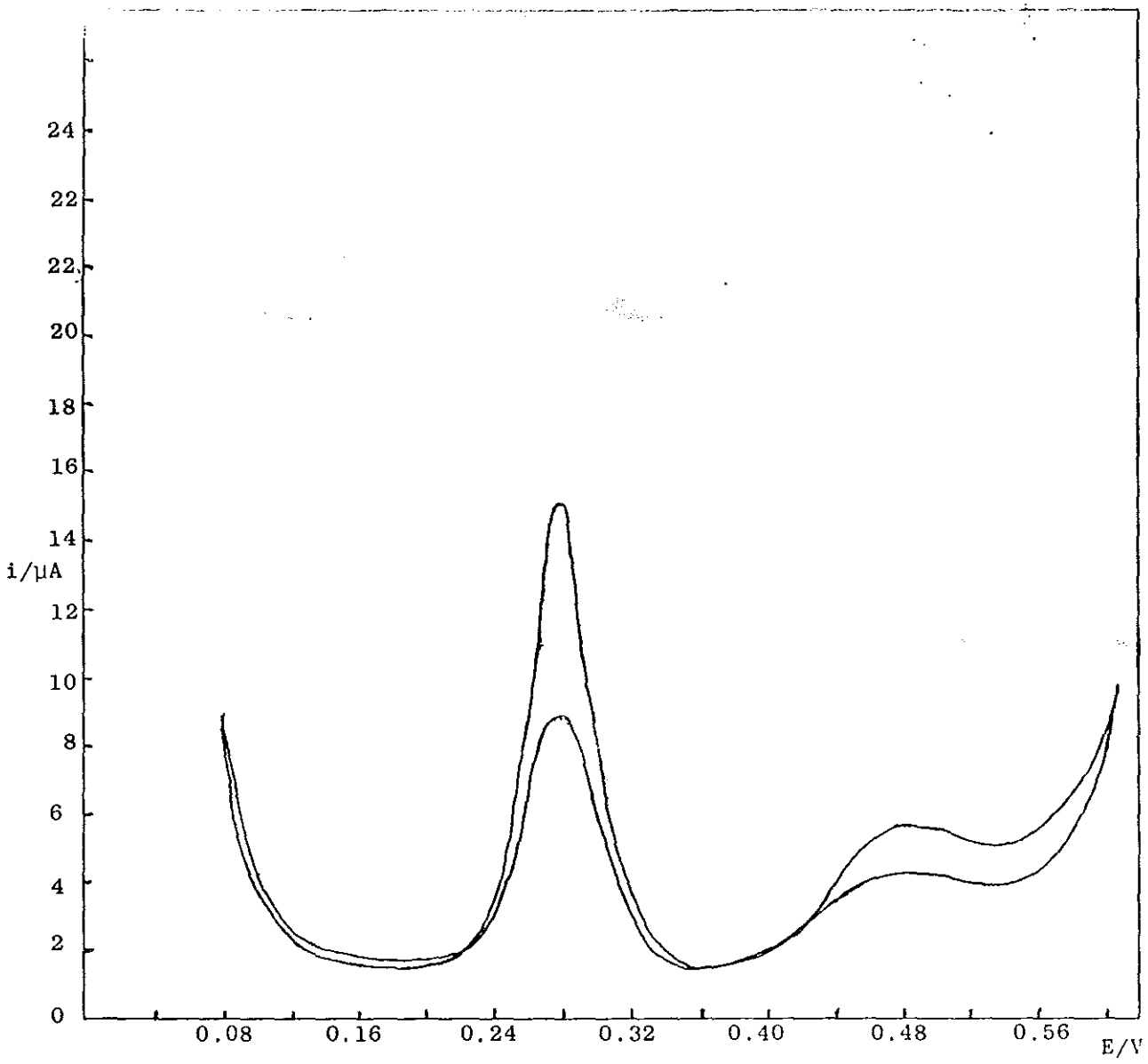

Fig. 13 AC cyclic voltammogram for the facilitated transfer o
Fe(II). Aqueous phase 1mM FeSO4 in 10mM MgSO4. Organic phase 10 m
2,2'-dipyridine + 10 mM CVTPB in nitrobenzene. f=35Hz, sweep rat
12mv/sec.

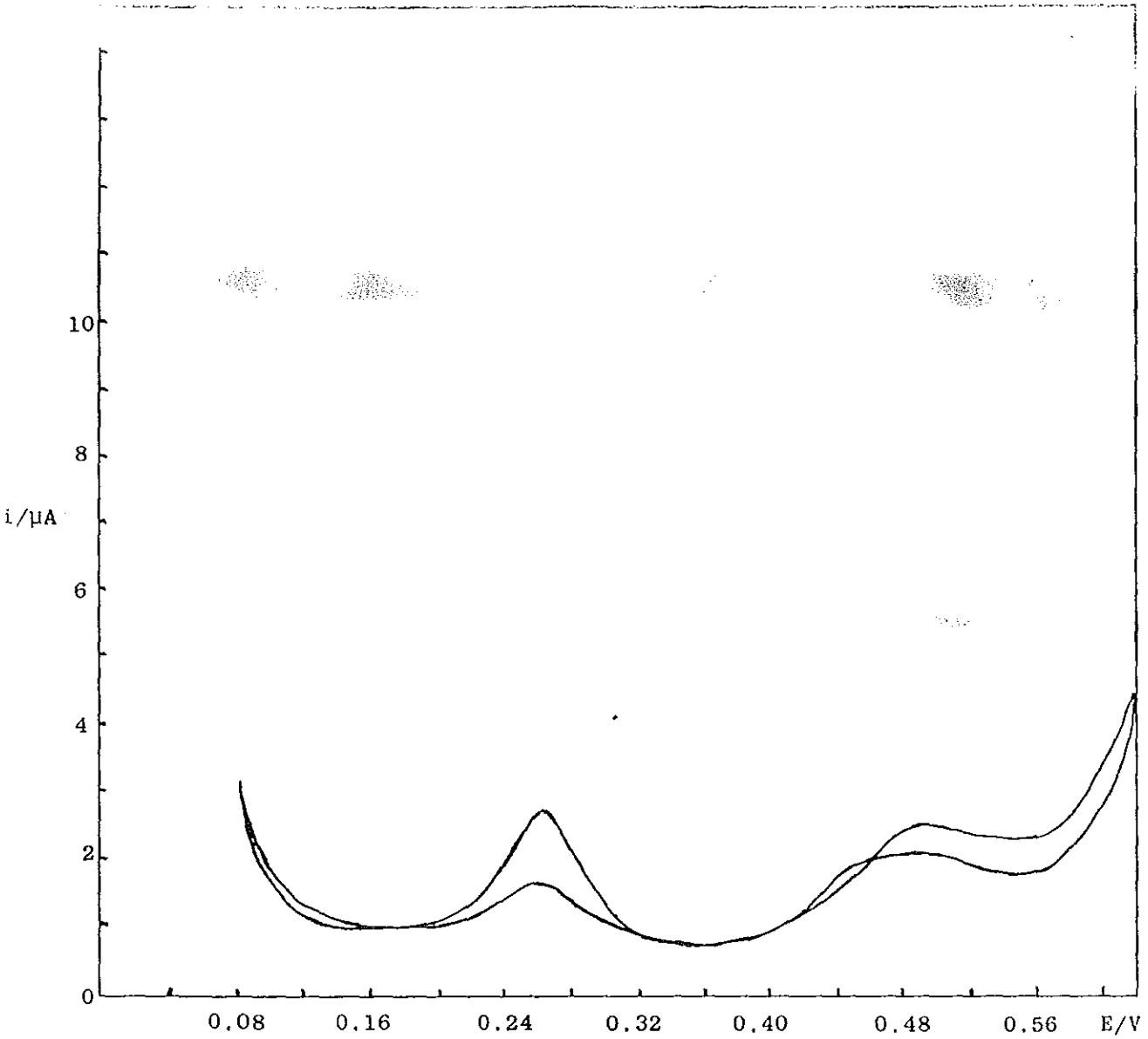

Fig. 14 AC cyclic voltammogram for the facilitated transfer of Ni(II). Aqueous phase 10 mM NiSO4 in 10 mM MgSO4. Organic phase 10 mM 2,2'-dipyridine + 10mM CVTPB in nitrobenzene. f=35Hz, sweep rate 12mv/sec.

As can be seen from Fig. 15 the current peak magnitude is larger for the tris complex while the literature value of the stability constant is smaller than that of the bis complex. The magnitude of the peak current for Ni^{2+}-bipyridine bis and tris complexes are similar, in reasonable agreement with the literature values (Table 5).

When the solution of the metal ions (Fe^{2+} and Cd^{2+}) were first brought in to contact with the organic phase containing 2,2'-bipyridine, the peak at higher potential increased and decreased rapidly while the peak at lower potential (i.e. for the tris complex) increased steadily until a final value was reached. This shows that the transfer takes place by successive complexation of the metal ions. This was further confirmed by studying the transfer behaviour of these ions at different switching potentials. First the voltammogram was run in the potential range of the tris complex only and the peak current did not change with time; however, when the potential range was extended to where the bis complex transfer occurs the magnitude of the peak current of the tris complex increased. Therefore it can be concluded that the tris complex is formed from the bis complex by the addition of one 2,2'-bipyridine moiety when the bis complex is transferred to the organic phase.

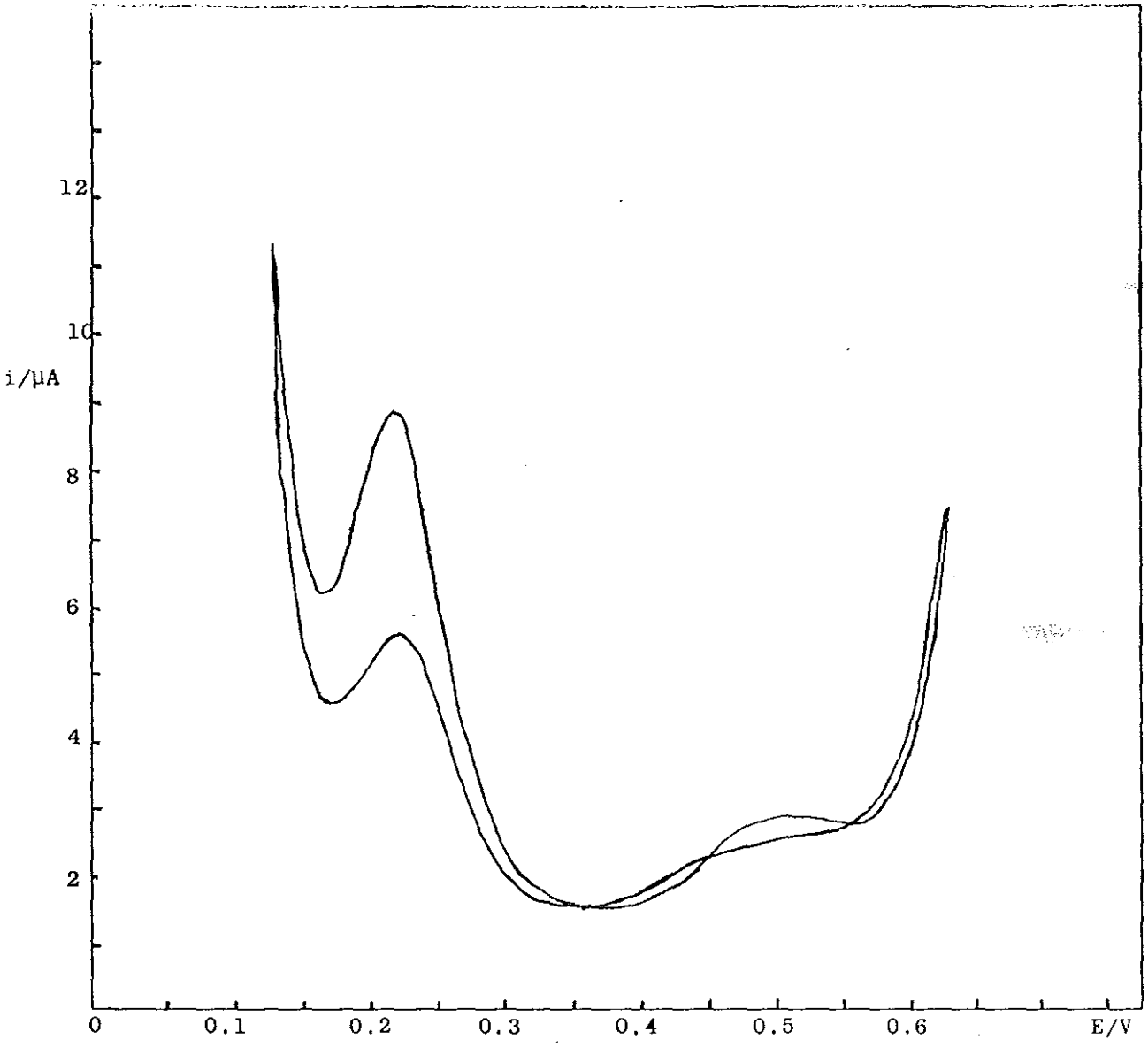

Fig. 15 AC cyclic voltammogram for the facilitated transfer of Cd(II). Aqueous phase 0.1 mM CdSO4 + 10 mM MgSO4; Organic phase 0.1 mM 2,2'-dipyridine + 10 mM CVTPB in nitrobenzene. f=35Hz, sweep rate 12mv/sec.

The transfer of the $Ni(bipy)_3^{2+}$ complex was also studied using single sweep voltammetry (Fig. 16). The current peak height versus the square root of sweep rate ($\upsilon^{1/2}$) (plotted in Fig. 17) showed a linear dependence up to υ= 150 mv/sec. This indicates the diffusion controlled transfer of the complexes up to a sweep rate of 150 mv/sec.Using the theory for linear potential sweep voltammetry at the stationary electrode [112], the diffusion coefficient $D_{Ni(bipy)3}2+$ in water was evaluated to be $2x10^{-6}$ cm^2/sec. from the peak currents corresponding to the transfer of $Ni(bipy)_3^{2+}$ from aqueous to the nitrobenzene phase. The value of the diffusion coefficient obtained by us was smaller compared with that of Homolka and Wendt ($7.5x10^{-6}$ cm^2/sec.) [96] in the membrane un-stabilized ITIES.This is clearly due to the slow diffusion inside the membrane.

For the case $C_M > C_L$ the half wave potential of Cd^{2+} facilitated transfer increased with decreasing metal ion concentration (Table 6). Evaluation of a stability constant was not possible because the mathematical treatment of the diffusion problem is complicated; in addition, since three complexes are formed the knowledge of at least two stability constants is required.

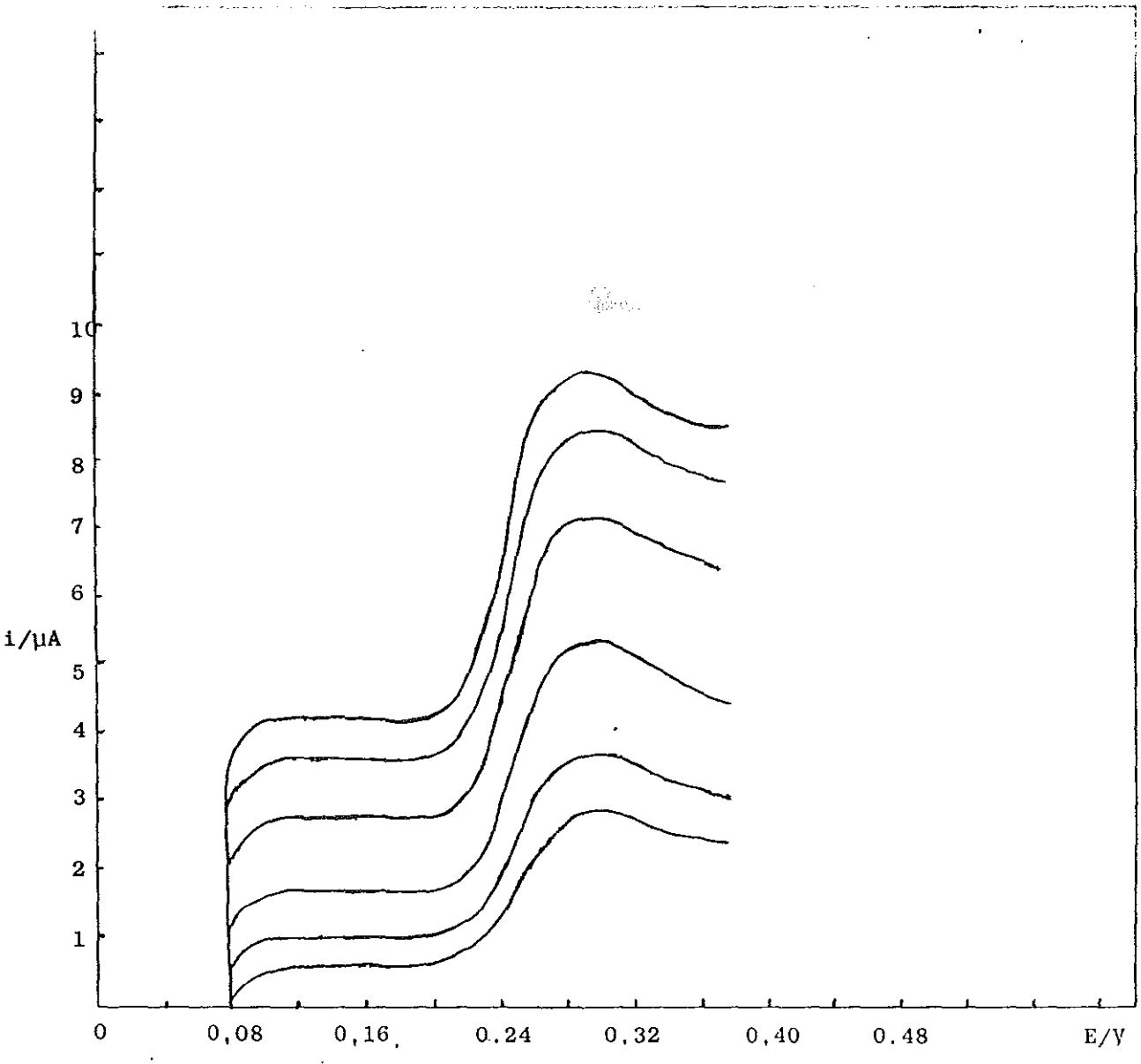

Fig. 16 Single sweep voltammograms for the transfer of $Ni(bipy)_3^{2+}$ complex at water/nitrobenzene interface. Aqueous phase 0.1 mM $Ni(bipy)_3^{2+}$ complex in 10 mM $MgSO_4$. Organic phase 10 mM 2, 2'-bipyridine + 10 mM CVTPB in nitrobenzene.

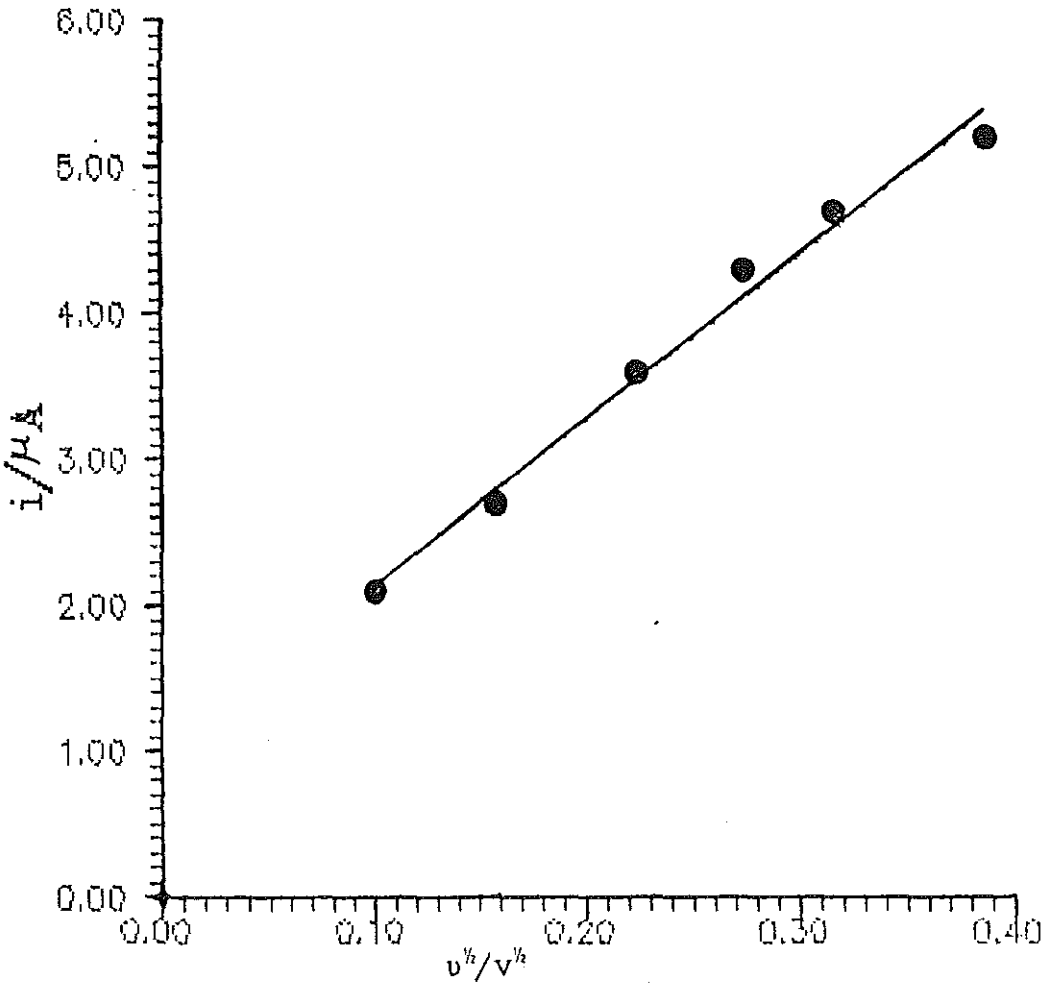

Fig. 17 Dependence of the peak current on the square root of sweep rate for the transfer of $Ni(bipy)_3^{2+}$ complex at the water nitrobenzene interface. Aqueous phase: 0.1mM $Ni(bipy)_3^{2+}$ complex in 10 mM MgSO4; Organic phase 0.1mM 2,2'-dipyridine + 10 mM CVTPB in nitrobenzene.

As can be seen from Table 6 the half wave potential was independent of the ligand concentration, for the case $C_H > C_L$ because the more stable tris complex is formed. On the other hand the facilitated transfer of Fe^{2+} with 2,2'-dipyridyl showed no shift in the half wave potential when the concentration of the metal ion (Fe^{2+}) was changed (see Table 7). We presume that the complexation reaction occurs at the interface. The difference in behavior between Cd^{2+} and Fe^{2+} could be attributed to the difference in their stability constants. The stability constant for Fe^{2+} with 2,2' bipyridine is 10^4 times greater than that of Cd^{2+} (Table 5).

Table 6 Dependence of $E_{1/2}$ on the concentration of Cd^{2+}. (The transfer of Cd^{2+} facilitated by 2, 2'-bipyridine dissolved in 10 mM CVTPB nitrobenzene).

Metal ion concentration/mM	$E_{1/2}$/mV
a) 0.1 mM 2, 2'-bipyridine (bis complex)	
0.10	560
1.00	525
10.0	500
b) 100 mM 2, 2'-bipyridine (tris complex)	
0.01	325
0.10	320

Table 7. Dependence of $E_{1/2}$ on the concentration of Fe^{2+}. (The transfer of Fe^{2+} facilitated by 2, 2'-bipyridine dissolved in 10mM CVTPB nitrobenzene, tris complex).

Metal ion concentration/mM	$E_{1/2}$/mv
a) 0.1 mM 2, 2'-bipyridine	
0.10	330
1.00	325
10.0	325
b) 100 mM 2, 2'-bipyridine	
0.01	325
0.10	320

Based on our general experimental observations we propose the following reaction scheme for Fe^{2+} and Ni^{2+} facilitated transfer.

Surface reactions $M(w) + L(o) \rightleftharpoons ML(w)$

$ML(w) + L(o) \rightleftharpoons ML_2(w)$

$ML_2(w) + L(o) \rightleftharpoons ML_3(w)$

Partition equilibria $ML(w) \rightleftharpoons ML(o)$

$ML_2(w) \rightleftharpoons ML_2(o)$

$ML_3(w) \rightleftharpoons ML_3(o)$

Before the start of the electrochemical experiment all species are present at low concentrations and we assume that ML(w) is the dominant species.On sweeping the potential in the positive direction the complex ions are transferred in the order of their respective sizes: first ML_3^{2+}, then ML_2^{2+} and ML^{2+} at the most positive potential. Because of the high concentration of ligand

in the organic phase the ML_3^{2+} concentration will increase continuously from cycle to cycle while the ML_2^{2+} concentration passes through a maximum.

Ac voltammetric studies of the facilitated transfer of Ni^{2+}, with 0.1 mM 2,2'bipyridine showed no peak even at higher concentrations of the metal ion. This could be due to the slow reaction kinetics discussed previously. Yoshida & Freiser [118] observed similar behavior, when they were studying the kinetics of the transfer of Ni^{2+} facilitated by the stronger ligand 1,10 phenathroline. They observed no peak, for the transfer of Ni-(phen)$^{2+}$ complex, even at a higher Ni^{2+} concentration (10 mM).

The transfer of the complexed ion, $Ni(bipy)_3^{2+}$, showed no shift of the half wave potential when the concentration was changed. And the peak current increased with increasing concentration of the complex in agreement with theory.

The half-wave potential for the facilitated transfer of Ni^{2+}, Fe^{2+} and Cd^{2+}, evaluated using perchlorate as a reference ion, are given in the following Table.

Table 8. Half-wave potentials (of the tris complex) for the transfer of 1mM Ni^{2+}, Fe^{2+} and Cd^{2+} facilitated by 10mM 2,2'-bipyridine.

Metal ion	$\Delta_o^w\varphi_{1/2}$/v
Ni^{2+}	-0.208
Fe^{2+}	-0.215
Cd^{2+}	-0.175

Another important result is the peak separation between the successive complexes. For Ni^{2+} and Fe^{2+} the peak separation between the bis and tris complex was similar ($\Delta E \approx$ 0.2v). This amounts to a change in the standard Gibbs energy of transfer between the successive complexes, $\Delta\Delta G^{\circ}_{tr}$, of 38.6 kJ/mol. In their studies of Ni-bipy complex ion transfer, Homolka and Wendt [96] found equally separated peaks (between $Ni(bipy)^{2+}$, $Ni(bipy)_2^{2+}$ and $Ni(bipy)_3^{2+}$) by about $\Delta E \approx 0.17$v ($\Delta\Delta G^{\circ}_{tr}$= 33 kJ/mol). This change in standard Gibbs energy of transfer is brought about by the replacement of two water molecules by one 2,2'-bipyridine molecule. The higher $\Delta\Delta G^{\circ}_{tr}$ in our case, compared with that of Homolka and Wendt, could be due to the slow diffusion inside the membrane [9]. The peak separation for Cd^{2+}-bipy complexes, however, was much bigger, $\Delta E \approx 0.275$ v ($\Delta\Delta G^{\circ}_{tr} \approx 53$ kJ/mol) and the details of the transfer mechanism should be studied further.

6. CONCLUSION

The transfer of Cd^{2+} and Fe^{2+} facilitated by 2,2'-bipyridine and the complex ion transfer of $Ni(bipy)_3^{2+}$ were studied using flow injection analysis. The transfer of these ions is reversible and diffusion controlled. On the other hand the transfer of Ni^{2+} facilitated by 2,2'-bipyridine is kinetically controlled.

In the facilitated transfer of the divalent transition metal ions the transfer of the bis and tris complexes were within the potential window of the ac and dc cyclic voltammogram. The peak at lower potential is presumed to be due to the tris complex while that at the higher potential to be due to the bis complex. The transfer mechanism for Fe^{2+} and Ni^{2+}, with 2,2'-bipyridine in nitrobenzene, appears to be a complex ion transfer while that of Cd^{2+} seems to be a facilitated ion transfer. Further study is required to elucidate the transfer mechanism of Cd^{2+} and to explain the high value of the change in standard Gibbs energy of transfer between the tris and bis complexes (53 KJ/mol). For Ni^{2+} and Fe^{2+} the change in standard Gibbs energy of transfer between the successive complexes is in reasonable agreement (38.6 KJ/mol) with the reported values (33 KJ/mol).

7. REFERENCES

1. H.H. Girault D.J. Schiffrin in A.J. Bard (Ed), Electroanlytical Chemistry, vol. 15, Marcel Dekker Inc., New York, 1989.

2. J. Koryta, Electrochim Acta, 24 (1979) 293.

3. J. Koryta, Electrochim. Acta, 32 (1987) 419.

4. B. Hundhammer, S.K. Dhawan, A. Bekele and M.J. Seidlitz, J. Electroanal. Chem., 217 (1987) 253.

5. J. Koryta, Electrochim. Acta, 29 (1984) 445

6. V. Marecek and Hanchenova, J. Electroanal. Chem., 217 (1987) 213.

7. B. Hundhammer and S. Wilke, J. Electroanal. Chem., 266 (1989) 133.

8. F. Ruixi and w. Xiaoping, J. Electroanal. Chem., 261 (1989) 77.

9. Mulat Abegaz, M. Sc. Thesis, Addis Abeba University, 1990.

10. B. Hundhammer, H. J. Seidlitz, S. Becker, S.K. Dhawan and T Solomon, J. Electroanal. Chem., 180 (1984) 355.

11. T. Kakiuchi, I. Obi and M. Senda, Bull. Chem. Soc. Jpn., 58 (1985) 1636.

12. H. Freiser, Chem. Rev. 88 (1988) 611.

13. E. W. Dehmlow, Angew. Chem. Int. Ed. Engl. 16 (1977) 493

14. Hailemichael Alemu, Ph.D. Dissertation, Addis Abeba University, 1991.

15. F. M. Karpfen and J.E.B. Randles, Trans. Faraday Soc., 49(1953) 823.

16. K. Sollner and G.M. Shean, J. Am. Chem. Soc., 86 (1964) 1901.

17. P. Vanysek, Electrochemistry on Liquid/Liquid Interfaces. "Lecture Notes in Chemistry", Springer-Verlag, Berlin, 1985.

18. M. Dupeyrat and J. Gusatalla J. Chim. Phys., 53 (1956) 469. As cited in ref. 17.

19. J. Guastalla J. Chim. Phys., 53 (1956) 470. As cited in

ref.17.

20. M. Blank, J. Colloid Interface Sci., 22 (1966) 53. Chem. Abst., 65 (1966) 97736.

21. C. Gavach, T. Mlondnicka and J. Guastalla, C.R. Acad. Sci. Paris. 266 (1968) 1196. Chem. Abst., 69 (1968) 7815.

22. J. Guastalla, Nature, 227 (1970) 485.

23. C. Gavach and F. Henry, J. Electroanal. Chem., 54 (1974) 361.

24. C. Gavach and B. D'Epenoux, J. Electroanal. Chem., 55 (1974) 59

25. C. Gavach, B. D'Epenoux and F. Henry, J. Electoanal. Chem., 64 (1975) 107.

26. C. Gavach, P. Seta and F. Henry, Bioelectrochem. Bioenerget., 1 (1974) 329.

27. J. Rais, Collect. Czech. Chem. Commun., 36 (1971) 269.

28. B. Hundhammer and T. solomon, J. Electroanal. Chem., 15 (1983) 19.

29. M. H. Abraham and J. Liszi, J. Inorg. Nucl. Chem., 43 (1981) 143.

30. M. H. Abraham & J. Liszi, J. Chem. Soc. Faraday Trans. I, 74 (1978) 1604.

31. Z. Koczorowski and G. Geblewicz, J. Electroanal. Chem., 108 (1980) 117.

32. T. Solomon, H. Alemu and B. Hundhammer, J. Electroanal. Chem., 169 (1984) 303.

33. Z. Samec, V. Homolka, V. Marecek and L. Kavan, J. Electoanal. Chem., 145 (1983) 213.

34. Z. Koczorowski, Z. Geblewicz and I. Paleska, J. Electroanal. Chem., 172 (1984) 327.

35. Z. Koczorowski, I. Paleska and Z. Geblewica, J. Electoanal. Chem., 164 (1984) 201.

36. T. Solomon, H. Alemu and B. Hundhammer, J. Electoanal. Chem., 169 (1984) 311.

37. B. Hundhammer, T. Solomon and B. Alemayheu, J. Electroanal Chem., 135 (1982) 301.

38. G. Geblewicz, A.K. Kontturi, K. Kontturi and D.J. Shiffrin, J. Electoranal. Chem., 217 (1987) 261

39. Z. Samec, V. Marecek, and J. Weber, J. Electroanal. Chem., 100 (1979)841.

40. B. Hundhammer, T. Solomon, and H. Aemu, J. Electroanal. Chem., 149 (1983) 179.

41. Z. Yoshida, and H. Freiser. J. Electroanal. Chem., 162 (1984)307.

42. H. H. Girault, D. J. Schiffrin, and B. Smith, J. Electroanal. Chem., 137 (1982) 207.

43. J. Koryta, P. Vanysek, and M. Brezina, J. Eectroanal. Chem., 67 (1976) 263.

44. G. Geblewicz, Z. Figaszewski, and Z. Koczorowski, J. Electroanal. Chem., 177 (1984) 1.

45. V. Marecek and Z. Samec, J. Electroanal. Chem., 149 (1983) 185.

46. J. D. Reid, O. Melroy, and R. Buck, J. Electroanal. Chem., 147 (1983) 71.

47. C. Gavach, P. Seta, and B. D'Epenoux, J. Electroanal. Chem., 83 (1977) 225.

48. D. Homolka, K. Holub, and V. Marecek, J. Electroanal. Chem., 138 (1982) 29.

49. Z. Samec, J. Electroanal. Chem., 111 (1980) 211.

50. Z. Samec, V. Marecek, J. Weber, and D. Homolka, J. Electroanal. Chem., 126 (1981) 105.

51. T. Kakutani, T. Osaki and M. Senda, Bull. Chem. Soc. Jpn., 56 (1983) 991.

52. D. Homolka, V. Marecek, Z. Samec, and K. Base, J. Electroanal. Chem., 163 (1984) 159.

53. Mekuria Habteyohannes, M.Sc. Thesis, Addis Ababa University, 1993.

54. V. Marecek and Z. Samec, Anal. Chim. Acta, 141 (1982) 65.

55. O. Dvorak, V. Marecek, and Z. Samec., J. Electoanal. Chem., 284 (1990) 205.

56. P. Seta, B. D'Expenoux, and C.Gavach, J. Electroanal. Chem., 95 (1979) 191.

57. T. Kakiuchi and M. Senda, Bull. Chem. Soc. Jpn., 56 (1983) 1322.

58. H. H. Girault and D. J. Schiffrin., J. Electroanal. Chem., 150 (1983) 43.

59. P. Hajkova, J. Electroanal. Chem., 225 (1987) 65.

60. D. Homolka, P. Hajkova, V. Marecek, and Z. samec, J. Electroanal. Chem., 159 (1983) 233.

61. Z. Samec, V. Marecek, and D. Homolka, Farad. discuss. Chem. Soc., 77 (1984) 197.

62. T. Osaki, T. Kakutani, and M. Senda, Bull. Chem. Soc. Jpn., 57 (1984) 370.

63. Z. Samec, Y. Marecek, and D. Homolka, J. Electroanal. Chem., 187 (1985) 31.

64. G. M. Torrie and J. P. Yalleau, J. Electroanal. Chem., 206 (1986) 69.

65. Z. Samec, Chem. Rev., 88(1988) 617.

66. C. W. Quthnaite, L. B. Bhuiyan, and S. Leving, J. Chem. Soc. Farad. Trans. II, 76 (1980) 1388.

67. Z. Samec, V. Marecek, and D. Homolka, J. Electroanal. Chem., 170 (1984) 383.

68. Z. Samec and V. Marecek, J. Electroanal. Chem., 200 (1986) 17.

69. T. Osaki, T. Kakutani, and M. Senda, Bull. Chem. Soc, Jpn., 58 (1985) 2626.

70. Z. Samec, D. Homolka, and V. Marecek, J. Electroanal. Chem., 135 (1982) 265.

71. T. Kakutani and Y. Nishiwaki, Bull. Chem. Soc. Jpn., 59 (1986) 781.

72. H. H. Girault and D. J. Schiffrin, J. Electroanal. Chem., 15 (1985) 213.

73. R. P. Buck and W. E. Bronner, J. Electroanal. Chem., 197 (1986) 179.

74. Z. Samec, V. Marecek, J. Weber, and D. Homolka, J. Electronal. Chem., 99 (1979) 385.

75. P. Vanysek and M. Behrend, J. Electroanal. Chem., 130 (1981) 287.

76. D. Homolka, L.Q. Hung, A. Hofmanova, M. W. Kahlil, J. Koryta, V. Marecek, Z. Samec, S. K. Sen, P. Vansek, J. Weber, M. Brezina, M. Janda, and I. Stebor, Anal. Chem., 52 (1980) 1606.

77. Z. Koczorowski and G. Geblewicz, J. Electroanal. Chem., 152 (1983) 55.

78. G. Geblewicz and Z. Koczorowski, J. Elecroanal. Chem., 158 (1983) 37.

79. Z. Samec, V. Marecek, and M. P. colombini, J. Electroanal. chem., 257 (1988) 147.

80. E. Makrlik and L.Q. Hung, J. Electroanal. Chem., 158 (1983) 269.

81. J. Koryta, P. Vanysek and M. Brezina. J. Electroanal. Chem., 75 (1977) 211.

82. P. Vanysek, J. Electroanal. Chem., 121 (1981) 149.

83. S. Kihara, M. Suzuki, K. Meada, K. Ogura, and M. Matsui, J. Electroanal. Chem., 210 (1986) 147.

84. Z. Pang and E. Wang, J. Electroanal. Chem., 252 (1988) 245.

85. E. Wang and Z. Sun, J. Electroanal. Cem., 220 (1987) 235.

86. V. Marcek and M. P. Colombini, J. Electroanal. Chem., 241 (1988) 133.

87. P. Vanysek, W. Ruth and J. Koryta, J. Electroanal. Chem., 148 (1983) 117.

88. A. Hofmanova, L. Q. Hung and W. Kahlil, J. Electroanal. Chem., 135 (1982) 257.

89. Z. Yoshidla and H. Freiser, J. Electroanal. Chem., 179 (1984) 31.

90. L. Sinru and H. Freiser, J. Electroanal. Chem., 191 (1984) 437.

91. L. Sinru, Z. Zaofan, and H. Freiser, J. Electroanal. Chem., 210 (1986) 137.

92. G. Taylor and H. H. Girault, J. Electroanal. Chem., 208 (1986) 179.

93. V. Marecek and Z. Samec., Anal. Chem. Acta, 151 (1983) 265.

94. D. Homolka, V. Marecek and Z. Samec, J. Electroanal. chem., 125 (1981) 243.

95. D. Homolka, K. Holub and V. Marecek, J. Electroanal. Chem., 138 (1982) 29.

96. D. Homolka and H. Wendt, Ber. Bunsenges. Phys. Chem., 89 (1985) 1083.

97. E. Wang and Y. Liu, J. Electroanal. Chem., 214 (1986) 465.

98. Y. Liu and E. Wang, J. Electroanal. Chem., 277 (1990) 305.

99. Z. Yoshida and S. Kihara, J. Electroanal. Chem., 227 (1987) 171.

100. G. Du, J. Koryta, W. Ruth and P. Vanysek, J. Electoanal. Chem., 159 (1983) 413.

101. D. Homolka, V. Marecek, Z. Samec, K. Base and H. Wendt, J. Electroanal. Chem., 163 (1984) 159.

102. N. Ogawa and H. Freiser, Anal. Chem., 65 (1993) 517.

103. E. Grunwald, G. Baughman and G. Kohnstam, J. Am. Chem. Soc., 82 (1960) 5801.

104. L. Q. Hung, J. Electroanal. Chem., 115 (1980) 159.

105. M. A. Abraham and J. Liszi, J. Chem. Soc. Faradsy Trans. I, 74 (1978) 2858.

106. M. A. Abraham, J. Liszi and L. Meszros, J. Chem. Phys., 70 (1979) 2491.

107. M. A. Abraham and J. Liszi, J. Chem. Soc. Faraday Trans. I, 76 (1980) 1219.

108. M. A. Abraham, J. Liszi, and E. Papp, J. Chem. Soc. Faraday Trans. I, 78 (1982) 197.

109. A.M. Bond and J. O'Halloran, Anal. Chem., 48 (1976) 872.

110. A.M. Bond and J. O'Halloran, Anal. Chem., 50 (1978) 216.

111. Merid Tessema, M. Sc. Thesis, Addis Ababa University, 1990.

112. R. S. Nicolson and I. Shain, Anal. Chem., 36 (1964) 706.

113. P. W. Delahy, New Instrumental Methods in Electrochemistry. Intersince, New York, 1954.

114. H. Gunasingham and B. Fleet, Anal. Chem., 55 (1983) 1409.

115. B. Hundhammer, T. Solomon, T. Zerihun, M. Abegaz and A. Bekele, to be published.

116. H. Irving and D.H. Mellor, J. Chem. Soc., (1962) 5222.

117. R. H. Holyer, C. D. Hubbard, S. F. A. Kettle, R. G. Wilkins, Inong. Chem., 4 (1965) 929.

118. Z. Yoshida and H. Freiser, Inorg. Chem., 23 (1984) 3931.

119. F. Basolo and R.G. Pearson, Mechanism of Inorganic Reactions. A Study of Metal Complexes in Solution, John Wiley, New York, 1968.

120. A.E. Martell (Ed) , Coordination Chemistry, Vol.2, ACS Monograph 174, Washington, D.C., 1978.